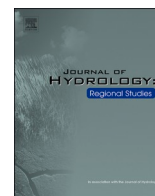


Contents lists available at [ScienceDirect](https://www.sciencedirect.com)

## Journal of Hydrology: Regional Studies

journal homepage: [www.elsevier.com/locate/ejrh](http://www.elsevier.com/locate/ejrh)

# A temporal snapshot of ecosystem functionality during the initial stages of reclamation of an upland-fen complex

Nataša Popović<sup>\*</sup>, Richard M. Petrone, Adam Green, Myroslava Khomik, Jonathan S. Price

Department of Geography & Environmental Management, University of Waterloo, Waterloo, Ontario N2L 3G1, Canada

## ARTICLE INFO

## Keywords:

Ecosystem function  
Net ecosystem exchange  
Reclamation  
Water-use efficiency  
Eddy covariance  
Boreal

## ABSTRACT

**Study region:** Athabasca River Watershed, Athabasca Oil Sands Region (AOSR), Alberta, Canada.  
**Study focus:** AOSR pre-disturbance landscape consists of a mosaic of upland-peatland complexes, dominated by fens, which have become the focus of recent mandatory reclamation efforts. Quantifiable metrics for evaluating reclamation project trajectories and long-term sustainability are required. Here, the initial performance of a constructed upland-peatland complex (Nikanotee Fen Watershed) is evaluated through a functional-based, ecosystem-scale approach focused on carbon dynamics and water use efficiency (WUE). Initial seven years (2013–2019) post-construction were monitored using eddy covariance and multispectral imagery to capture ecosystem evolution.

**New hydrological insights for the region:** Results indicate the fen quickly evolved from a bare-ground, carbon source (2013) to a sedge-dominated (*Carex aquatilis*), carbon sink (2015). Slower growth rate of trees (*Pinus banksiana*, *Populus balsamifera*) and dry edaphic upland conditions initially resulted in net carbon losses. However, as upland vegetation became established, plant CO<sub>2</sub> uptake increased. After 2015, fen WUE remained relatively stable despite fluctuations in seasonal rainfall. Stable WUE reflects a well-connected groundwater network between the two landscape units that supports hydrological self-regulation sufficient to maintain adequate plant function. Because of this groundwater supply, fen plants were no longer dependent solely on precipitation – increasing resilience to intervals of periodic water stress. Overall, carbon and water dynamics during early-development suggests the system is evolving towards a self-sustaining, carbon-accumulating, functional ecosystem.

## 1. Introduction

The Western Boreal Plains (WBP) ecozone provides important economic (via natural resource extraction) and environmental ecosystem services (EES) on regional and global scales. EES provided by landscapes in the region include: the regulation of regional hydrological regimes; providing niche, diverse ecosystems; nutrient transformation through biogeochemical cycling; and perhaps most importantly, carbon sequestration and long-term carbon storage in soils (Lamothe et al., 2018; Kurz et al., 2013; Yu, 2012; Limpens et al., 2008; Blodau, 2002). The Athabasca Oil Sands Region (AOSR) encompasses an area of 93,259 km<sup>2</sup> within the WBP of north-eastern Alberta, of which 5% (4800 km<sup>2</sup>) is considered minable for oilsands extraction (ABMI, 2017). Here, one method of resource

<sup>\*</sup> Corresponding author.

E-mail address: [npopovic@uwaterloo.ca](mailto:npopovic@uwaterloo.ca) (N. Popović).

<https://doi.org/10.1016/j.ejrh.2022.101078>

Received 15 August 2021; Received in revised form 11 March 2022; Accepted 4 April 2022

Available online 9 April 2022

2214-5818/© 2022 The Authors. Published by Elsevier B.V. This is an open access article under the CC BY-NC-ND license (<http://creativecommons.org/licenses/by-nc-nd/4.0/>).

extraction consists of widespread surface mining, where up to 75 m of substrate below the ground surface are removed, resulting in a fully altered, disturbed landscape and subsequent loss of vital EES (Nwaishi et al., 2015a). Notably, Rooney et al. (2012) estimate AOSR mining activities will result in a potential net loss of 11.4 – 47.3 Tg of stored soil carbon. As of 2016, 901 km<sup>2</sup> of land in the AOSR has been impacted by mining activities. (Government of Alberta, 2017b). Companies operating in the AOSR have a statutory obligation to return leased land to pre-disturbance equivalent land capability, defined as post-reclamation landscapes that can support ecosystem services and functions similar to what existed prior to disturbance (Alberta Environment, 2008). However, the resulting reclaimed landscape may not necessarily be identical to the pre-disturbance landscape (Poscente and Charette, 2011; Alberta Environment, 2008). As reclamation efforts in the region typically use mine waste materials (i.e., tailing sand, petroleum coke) as construction substrates, the trajectory and end-result of reclaimed systems is likely to result in a hybrid, or novel landscape. These landscapes may be physically different, but functionally similar to natural, pre-disturbance landscapes as the structural and hydrogeochemical characteristics of construction materials used in AOSR reclamation endeavours are vastly different than those found in natural systems (Nwaishi et al., 2015a; Daly et al., 2012). The pre-disturbance landscape of the AOSR comprises a mosaic of upland forests (23%) and wetlands (54%) (AEP, 2018; Rooney et al., 2012), which are largely fen peatlands (Daly et al., 2012; Chee and Vitt, 1989). Initially, reclamation endeavours in the AOSR focused solely on reclaiming to upland forests. However, due to the extensive occurrence of peatlands, their specific ecosystem services (i.e., carbon storage) and hydrologic interconnectivity between uplands and peatlands, fens have begun to be integrated into regional reclamation efforts (Ketcheson et al., 2016). Due to the magnitude of disturbance, reclamation endeavours require the complete reengineering of surface topography and subsurface stratigraphy in addition to the initiation of vegetation through planting campaigns.

Reestablishment of hydrological connectivity is critical to the evolution and success of reclaimed landscapes, due to water requirements of key ecohydrological and biogeochemical functions – particularly in peatlands (i.e., inundated conditions, stable, near surface water table; Daly et al., 2012; Elshorbagy et al., 2005). Ensuring adequate water for ecosystem function in the AOSR is further complicated by the sub-humid climate of the region, where annual evapotranspiration commonly exceeds precipitation, resulting in frequent periods of water stress (Bothe and Abraham, 1993). Moreover, this water stress is expected to worsen in the area according to climate projections (Thompson et al., 2017; Ireson et al., 2015; Devito et al., 2012). The availability (and use) of water in an ecosystem is critical to successful development and function and is controlled mainly by the storage capacity of soils and vegetation (Rodríguez-Iturbe and Porporato, 2004). Thus, reclamation design in the AOSR needs to ensure adequate water availability for successful ecosystem development and function while accounting for the limited water availability.

The overarching goal of reclamation in the region is to create functional, self-sustaining, resilient ecosystems. As such, benchmarks encompassing ecologic, hydrologic and industry perspectives of ecosystem performance have been defined (Daly et al., 2012) and successful reclamation requires an ecosystem to be: (1) capable of supporting a representative assemblage of species; (2) carbon accumulating; and (3) able to withstand periodic environmental stress.

As AOSR fen reclamation is a relatively new endeavour, quantifiable metrics for evaluating the trajectory, success and long-term sustainability of reclamation projects is required. As it is difficult to directly measure ecosystem function through a single metric, the evaluation of reclamation performance has typically relied on the measurement of a large number of ecosystem variables (e.g., soil properties and geochemistry, vegetation surveys, biomass, water use), under the premise that in aggregate these variables will reflect ecosystem function and land capability. However, this approach has limitations, such as: data on a large number of variables can be onerous to collect and impossible to appropriately integrate; variables may be poor indicators of actual function; measured variables may reflect current site performance but fail to provide information on site stability under changing conditions, and on broader landscape-level performance. Alternatively, a focus on fewer biologically integrative factors or on emergent properties may be more effective (Straker et al., 2019; Strilesky et al., 2017; Nwaishi et al., 2015a).

Ecosystem water and carbon dynamics are integrative indicators of a suite of supporting ecosystem processes and characteristics. For example, water use efficiency (WUE), which links photosynthesis with water use, provides a useful metric to evaluate the use of water and carbon resources by plants. As such, assessment of the efficiency of ecosystem water use provides important insight on resiliency to climatic variation, and on landscape-level water storage and yield. Net ecosystem exchange (NEE) captures the net exchange (i.e., photosynthesis and respiration) of carbon between an ecosystem and the atmosphere and is a primary gauge of ecosystem carbon sink capacity. The overall carbon sink capacity of an ecosystem is dependent on edaphic conditions, water availability and plant community composition. Thus, integration of ecosystem-scale measurements of carbon exchange coupled with remote sensing metrics for plant development provides an efficient integrative measure of reclamation performance and early successional trajectory.

To date, only two pilot projects assessing reclamation design and performance have been constructed in the AOSR. Considerable research on early hydrological functioning (Biagi et al., 2021; Ketcheson et al., 2017), hydrochemistry (Biagi et al., 2019; Kessel et al., 2018; Simhayov et al., 2017), soil dynamics (Sutton and Price, 2020a, 2020b; Scarlett and Price, 2019; Gingras-Hill et al., 2018; Nwaishi et al., 2015b), ecology (Messner et al., 2019; Borkenhagen et al., 2019; Vitt et al., 2016) and plot-scale, seasonal carbon and water exchanges (Davidson et al., 2021; Scarlett et al., 2017; Nwaishi et al., 2016) has been conducted on reclaimed AOSR systems. However, there are limited long-term, assessments of performance based on ecosystem-scale metrics such as carbon and water dynamics in reclaimed, post-mining landscapes.

This study evaluates ecosystem development and performance during the initial stages of reclamation at the Nikanotee Fen Watershed (NFW; a constructed upland-fen complex) through the use of ecosystem scale techniques (e.g., eddy covariance towers, remote sensing). Specifically, the objectives were to: (a) provide a temporal snapshot of ecosystem evolution by using plant development, net ecosystem exchange (NEE) and WUE as metrics; (b) evaluate ecosystem functionality and (c) provide context to NFW performance through the comparison of carbon dynamics at surrounding natural and post-disturbance sites.

## 2. Study site

The Nikanotee Fen Watershed (NFW) is a 32-ha constructed watershed located within an oil sands mining operation approximately 30 km north of Fort McMurray, Alberta (56°55.944'N, 111°25.035'W; Fig. 1). NFW consists of three previously reclaimed slopes (18.7 ha), an undisturbed natural slope (2.8 ha), a newly reclaimed upland (7.7 ha) and fen peatland (2.9 ha). This study focuses only on the newly reclaimed upland and fen landscapes of the system (Fig. 1).

WBP climate is sub-humid, with thirty-year climate normals (1981–2010) having a mean July temperature of 17.1 °C, and an average of 419 mm of precipitation annually, of which ~70% occurs as rainfall (Environment Canada, 2015; Smerdon et al., 2008). Evapotranspiration (ET) commonly exceeds precipitation (P), resulting in periods of water stress (Petrone et al., 2007; Marshall et al., 1999; Bothe and Abraham, 1993).

NFW was designed based on numerical modelling of ideal geometries and substrate materials for successful ecosystem function within the WBP climate, while satisfying vegetation water requirements and facilitating peat accumulation (Price et al., 2010).

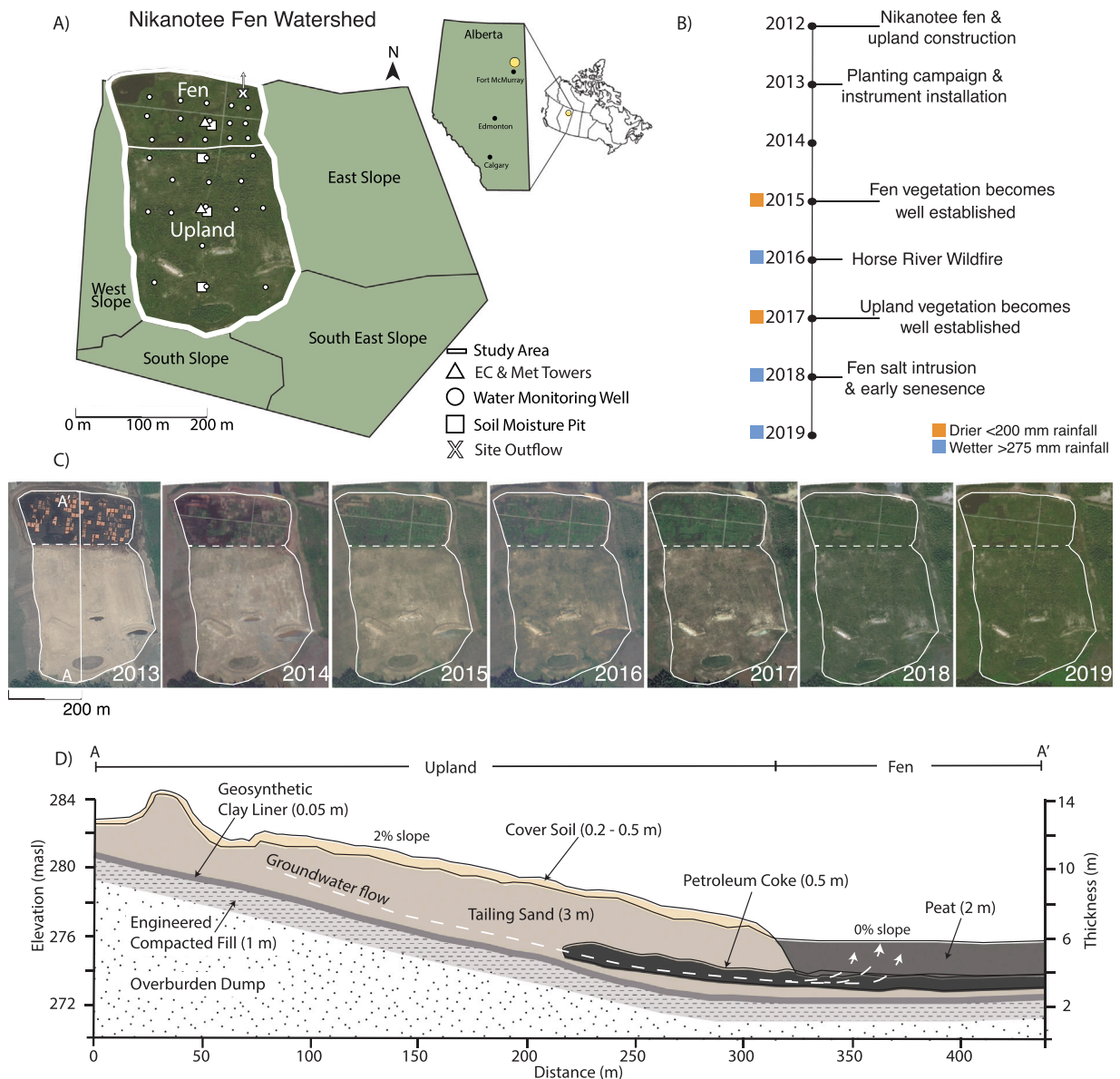


**Fig. 1.** A) Map of the Nikanotee Fen Watershed depicting the regions of interest (Fen and Upland) and the locations of soil moisture pits, eddy covariance and meteorological towers and water monitoring wells. B) Summary of key changes and milestones in site development over the first seven years following construction. C) Satellite imagery of site (plant) development. D) Stratigraphic cross-section along a central transect (A-A', shown in Fig. 1C-2013) depicting the layering of substrate materials and general groundwater flow direction. The thickness of each layer is indicated in parentheses. Note that the thickness of the clay liner in the diagram is not to scale (illustrated thicker than the actual 0.05 m thickness).

Moreover, the system is designed to function in a simplified, but analogous manner to fen-upland ecosystems common in undisturbed landscapes of the WBP, where uplands supply groundwater to downgradient peatlands (Wells et al., 2017; Elmes and Price, 2019). As such, there is no manual manipulation of the water table at NFW. Hydrological inputs to the system include precipitation and surface runoff from the surrounding, previously reclaimed hillslopes (Fig. 1 A) and fen hydrology is dependent on the down-gradient transport of water from the upland aquifer (Sutton and Price, 2020a; Ketcheson et al., 2016). Surface water is discharged through an outflow located in the northeastern corner of the fen. A complete account of NFW hydrological functioning is given in Ketcheson et al. (2017).

Construction of the upland-fen complex began in 2012 and concluded in January 2013. Planting and revegetation were initiated in June 2013. In 2014, additional peat was added to the fen, in an attempt to counter ponding, and additional tamarack seedlings were planted in the upland. The upland surface was subsequently modified through tillage to create furrows perpendicular to flow, to limit excessive overland flow, increase recharge to the upland aquifer, and better facilitate development of plant rooting architecture (Sutton and Price, 2020a; Gingras-Hill et al., 2018; Ketcheson et al., 2017; Daly et al., 2012). In June 2015, a subsequent upland planting campaign occurred to actualize desired stand density (~10,188 additional tree and shrub saplings; Gingras-Hill et al., 2018).

Materials used in construction included locally and readily available recovered materials from mining operations, such as by-products of the bitumen extraction process (tailing sand, petroleum coke) and salvaged overburden (peat and forest mineral soils) from the initial clearing of natural landscapes on oil sands leases (Daly et al., 2012). In addition to being abundantly available, these recovered materials were used as they had the appropriate hydrophysical properties for recreating the requisite hydrologic connectivity (Price et al., 2010). The constructed upland-fen complex is underlain by an impermeable, engineered geotextile clay liner (0.05 m thick), which encourages lateral flow while limiting deep water loss to the regional water table (Fig. 1D). Above the liner is a 0.5 m thick layer of tailing sand overlain by a 0.5 m thick layer of petroleum coke, which extends beneath the fen and partway into the upland, acting as a highly permeable underdrain to improve hydrological connectivity and more evenly distribute water and solute flows beneath the fen (Fig. 1D; Simhayov et al., 2017; Daly et al., 2012). The entire system was constructed on, and due to the clay liner is hydrologically isolated from, a fine-textured over burden dump (Fig. 1D).

In the upland, 2–3 m of tailing sand creates an aquifer to support transport of water from upland to fen due to its relatively high hydraulic conductivity (Sutton and Price, 2020a). However, these physical properties also result in poor moisture retention, which in turn impedes plant growth and development (Fung and Macyk, 2015). Moreover, as a by-product of bitumen extraction, tailing sand contains residual amounts of highly mobile solutes, namely sodium ( $\text{Na}^+$ ), amongst other constituents (Simhayov et al., 2017; Rezanezhad et al., 2012), which can affect water quality (Biagi et al., 2019; Kessel et al., 2018; Simhayov et al., 2017; Rezanezhad et al., 2012) and plant function and diversity (Vitt et al., 2020; Nwaishi et al., 2016; Pouliot et al., 2012; Trites and Bayley, 2009). As such, a capping layer of salvaged forest soil (LFH, sandy loam to loam) was placed on top of the tailing sand to better promote plant growth and function by limiting the degree of solutes in the rooting zone and improving rooting zone water retention (Naeth et al., 2013). Cover soil thickness is variable throughout the upland and ranges between 20 and 50 cm thick. Planting prescriptions followed procedures outlined by the Cumulative Environmental Management Association revegetation manual (Alberta Environment, 2008). Revegetation used native species common to WBP uplands such as black spruce (*Picea mariana*), jack pine (*Pinus bankstana*), willow (*Salix sp.*), Labrador tea (*Ledum groenladicum*), bunch berry (*Cornus stolonifera*), and bog cranberry (*Vaccinium oxycoccos*) and is classified as a 'b/d' ecosite - consisting of tree and shrub species (Beckingham and Archibald, 1996). The upland is characterized by its deep water table (~2 m bgs) and drier surface conditions (Table 1).

The fen consists of 2 m of donor peat salvaged from newly developed lease areas, which was well decomposed, and intentionally derived from lower horizons lacking living roots, seeds or rhizomes. The fen was revegetated using an experimental factorial design that included mulching and weeding treatments on plots that had control (bare), moss, seedlings, seedling and moss and seeds (Borkenhagen and Cooper, 2019). In anticipation of pulses of  $\text{Na}^+$ -rich upland water, planting prescriptions incorporated both freshwater and saline sedge and graminoid species (*Carex aquatilis* (water sedge), *Calamagrostis stricta* (narrow reed grass), *Juncus balticus* (wire rush), *Triglochin maritima* (seaside arrow grass)), as well as a combination of *Sphagnum* and brown moss species harvested from a local rich fen via the moss transfer method (Rocheffort et al., 2003). Ponds were not part of the original design, but the fen has had permanent standing water since 2013 and much of these ponded regions have become robust with invasive *Typha latifolia*. The fen is classified as a 'j' ecosite – rich fen dominated by sedge species (Beckingham and Archibald, 1996). In contrast to the upland, the fen is characterized as a much wetter environment with a near surface water table and high volumetric water content (Table 1). During the

**Table 1**

Soil and vegetation characteristics of the NFW fen and upland. Soil moisture and water table depths are mean values from 2013 to 2019.

	Fen	Upland
Size(ha)	2.9	7.7
Substrate(m)	2 m salvaged peat 0.5 m petroleum coke 0.5 m tailing sand	0.2 – 0.5 m salvaged forest floor material (LFH; cover soil)0.5 m petroleum coke 3 m tailing sand
Planted	June 2013	June 2013/July 2015
Dominant Species (as of 2019)	<i>Carex aquatilis</i> <i>Juncus balticus</i> <i>Typha latifolia</i> <i>Ptychostomum pseudotriquetrum</i>	<i>Populus tremuloides</i> <i>Populus balsamifera</i> <i>Picea mariana</i> , <i>Pinus banksiana</i>
Volumetric Soil Moisture (5 cm)(%)	84	20
Volumetric Soil Moisture (30 cm)(%)	87	32
Water Table Depth (cm bgs)	8	209

study period, NFW experienced several biophysical changes driven by autogenic and allogenic factors. Fig. 1B provides a summary of milestones in site development.

### 3. Methods

This study focuses on the upland and fen landscapes of the NFW system (Fig. 1) during the snow-free, growing season period (May – September; DoY 135–255,  $n = 120$  days) from time of construction (2013) to present (2019). Here, peak season is defined as end of June to early August (DoY 170 – 220), based on plant dynamics and meteorological trends. 2016 has limited data (covering only DoY 178 – 230 ( $n = 52$ ) in the fen and DoY 178 – 256 ( $n = 78$ ) in the upland) due to the Horse Creek wildfire evacuation that affected Fort McMurray and surrounding region.

#### 3.1. Micrometeorological setup

Both upland and fen meteorological systems had similar sensor configurations. Ground heat flux ( $Q_g$ ,  $Wm^{-2}$ ) was calculated using ground heat flux probes (HFT3; Campbell Scientific: Logan, Utah, USA) inserted horizontally at depths of 5 cm below the ground surface, several metres apart and facing south. Air temperature ( $T_{air}$ , °C) and relative humidity (rH, %) were measured using a Rotronic HC2S3 (Campbell Scientific: Logan, Utah, USA), while precipitation (P, mm) with a tipping bucket (Texas Instruments TR-525 M) placed within a clearing near the tower to avoid canopy and tower influences. Vapour pressure deficit (VPD, kPa) was calculated using saturated vapour pressure (es), actual vapour pressure (ea), relative humidity (rH) and air temperature ( $T_{air}$ ), (Howell and Dusek, 1995). Net radiation ( $Q^*$ ,  $Wm^{-2}$ ) was measured using a CNR4 (Kipp Zonen; Delft, Netherlands). All meteorological data was sampled at 1-minute intervals and averaged every 30-min on a CR1000 datalogger (Campbell Scientific: Logan, Utah, USA). Each site had coupled eddy covariance systems, consisting of a closed path  $CO_2/H_2O$  gas analyzer (LI-7200: LI-COR: Lincoln, Nebraska, USA) and 3D sonic anemometer (Windmaster Pro: Gill Instruments: Lymington, Hampshire, UK) from 2013 to 2014, and an open path  $CO_2/H_2O$  gas analyzer (LI-7500: LI-COR: Lincoln, Nebraska, USA) with a 3D sonic anemometer (CSAT3 3D: Campbell Scientific: Logan, Utah, USA) from 2015 to 2019. Half-hourly values of photosynthetically active radiation (PAR) were derived from measured incoming shortwave radiation (CNR4 (Kipp Zonen; Delft, Netherlands) using a numerical coefficient (Britton and Dodd, 1976) and the LakeMetabolizer package in RStudio (Winslow et al., 2016; R Core Studio, 2021). Due to developing vegetation in the upland, the height of the eddy covariance system increased from 2 m (2013–2017) to 3 m (2018–2019) to maintain representative flux footprints

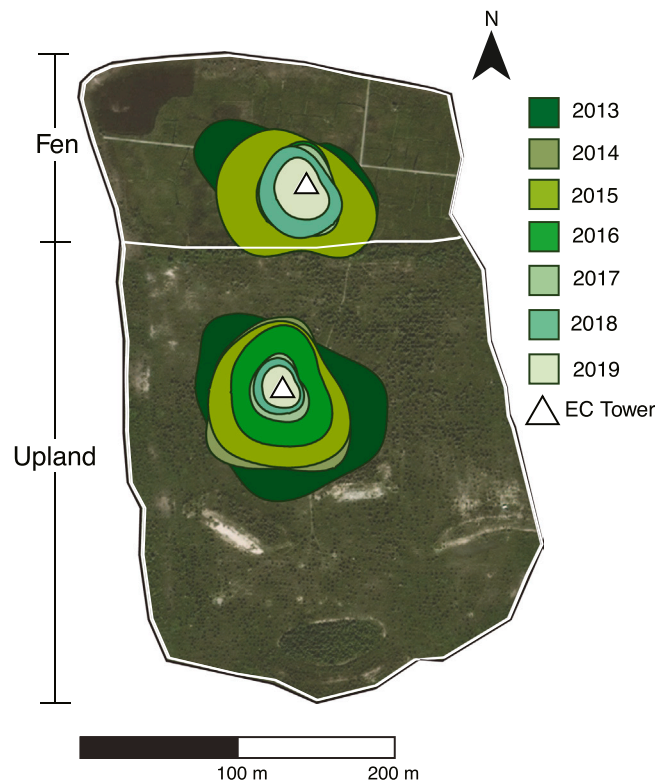


**Fig. 2.** Footprint of tower fetch for fen and upland from 2013 to 2019. Fetch decreases as the system develops. Increase in plant height results in an increase in surface roughness (thus, decrease in fetch). Note the similar extent of flux footprint in the fen from 2016 onwards once vegetation becomes stable.

(Fig. 2).

### 3.2. Eddy covariance data processing

Raw eddy covariance (EC) data were collected at 20 Hz and averaged every 30-min where corrections for coordinate rotation (double rotation; [Kaimal and Finnigan, 1994](#)), time lag and sensor separation ([Leuning and Judd, 1996](#)) and density effects ([Burba et al., 2012](#)) were applied, following common Fluxnet protocols ([Webb et al., 1980](#); [Leuning and Judd, 1996](#); [Foken and Leclerc, 2004](#); [Aubinet et al., 2012](#)). Resulting half-hour fluxes were then processed to ensure each half-hour flux record had 80% of the high-frequency records to maintain data quality. Data collected from open path systems (2015 – 2019) had additional filtering to remove periods that experienced precipitation or had the potential for dew formation on the infrared gas analyser lenses. Further outliers were removed by comparing a moving average for 10 half-hour means  $\pm 3$  standard deviations of neighbouring values, as well as comparing each half-hour for each year to remove any outliers that were outside of a  $\pm 3$  standard deviations. A final manual check was completed to remove any physically improbable values. The [Kljun et al. \(2004\)](#) footprint analysis was used to constrain the measured fluxes to be within 80% of the desired site boundaries; this was also used to determine flux distances used in this study (Fig. 2). Periods of low friction velocity ( $u^*$ ) were removed following methods outlined in [Wutzler et al. \(2018\)](#), using a 50%  $u^*$  threshold for all flux data. Filtered NEE were gap-filled using MDS method outlined in [Reichstein et al. \(2005\)](#) and then partitioned into respiration ( $R_{eco}$ ) and gross ecosystem production (GEP) using the relationship between night-time respiration and Tair ([Reichstein et al., 2005](#)). In this study, negative NEE indicates net ecosystem  $CO_2$  uptake from the atmosphere. Latent heat flux ( $Q_e$ ) was gap-filled by scaling potential evapotranspiration (PET) to actual evapotranspiration (AET) by calculating the ratio between AET and PET, where  $\alpha$  is the scaling variable, for each available half-hour. This ratio was then gap-filled using the MDS method outlined in [Reichstein et al. \(2005\)](#) where  $Q^*$ , VPD, and  $u^*$  were used as the gap-filling conditions. Sensible heat flux ( $Q_h$ ) was then gap-filled by solving the energy balance equation, using measured and gap-filled  $Q^*$ ,  $Q_e$  and  $Q_g$ . Water-use efficiency (WUE) was calculated as a ratio between gross ecosystem productivity (GEP) and AET ([Volk et al., 2021](#)).

### 3.3. Edaphic conditions and hydrometric network

Continuous measurements of volumetric water content (VWC) were collected at soil moisture pits along a north-south transect across both landscape units (three in upland, one in fen) (Fig. 1 A). VWC was measured over depths of 5 – 100 cm, however, only the 5, 15, 30 cm depths are reported here, as they represent the zone of most root biomass. Soil moisture pits were instrumented with dielectric impedance reflectometry soil moisture probes (Stevens Hydra Probe II) at each respective depth and recorded dielectric permittivity at one-minute intervals. Measurements were temperature and salinity corrected and converted to VWC based on a calibration ([Seyfried et al., 2005](#)) specific to the substrate material the probes were located in. Values were subsequently averaged to daily intervals. Soil temperature was measured at the meteorological stations using thermocouples (Type k thermocouple (2013–2018), CS-109 soil temperature probes (2019)) at 5 cm depth.

An extensive monitoring network of wells and piezometers was installed across NFW (Fig. 1). WTD was logged automatically through pressure transducers (HOBO MX2001-S, Onset, Massachusetts, USA) and coupled with weekly manual measurements. Wells were 2.54 cm inner diameter (I.D.) polyvinyl chloride (PVC) pipes that were fully slotted and wrapped with well screening ([Ketcheson et al., 2017](#)). Well depths were 1.5 m in the fen and 2.75 m in the upland (initially). In 2014, upland wells were lengthened to capture water table positions below 3 m.

### 3.4. Vegetation

#### 3.4.1. Field-based measurements

Leaf area index (LAI) was measured monthly along transects across both landscapes using LP-80 (2014–2018) and LI-2200 C (2019) LAI probes. Two readings were taken at each measurement location: one at, or near, the ground surface and another above the understory vegetation. This allowed LAI results to be calculated for the understory and canopy layers, as well as the sum total. LAI was corrected for canopy clumping, needle-to-shoot, woody-to-total area ratios, and sun-scattering effects ([Chen and Cihlar, 1996](#); [Chen et al., 1997](#); [Li-Cor, 2013](#)). The sparse nature of the upland canopy made it difficult to measure LAI of the canopy without large uncertainty and error. As such, LAI measurements are supplemented with other vegetation metrics to provide a more accurate description of vegetation characteristics.

Non-destructive vegetation surveys were conducted annually during peak growing season. In the fen, 60 × 60 cm collars installed for chamber-based  $CO_2$  flux measurements were used as the survey area ( $n = 32$ ), where percent cover of vascular plant species, litter, bare ground, and water were estimated, along with measurements of plant height and litter thickness. In the upland, tree surveys were completed using 10 randomly placed 10 m × 10 m plots, where species, height, and diameter at breast height (DBH) were measured. Trees less than 1.37 m in height were classified as saplings. Understory vegetation surveys were completed within these large plots ( $n = 5$  within each 10 × 10 plot), using a randomly placed 1 × 1 m quadrat.

#### 3.4.2. Enhanced vegetation index

Enhanced vegetation index (EVI) was derived to supplement field-based measurements and capture spatial and temporal vegetation development. While many vegetation indices are available (e.g., Normalised Difference Vegetation Index (NDVI); Red Edge Position (REP); Photochemical Reflectance Index (PRI) and EVI; see [Lees et al., 2018](#) for more details), EVI best fit the “open” canopy

nature of NFW, as it includes the blue band and background canopy correction, which helps better discern vegetation from wet, dark soils and leaf litter (Huete et al., 2002) - both of which are common in peatland settings. Additionally, EVI adjusts for atmospheric interference (clouds and aerosol particulates; Huete et al., 2002) and has been successfully applied in settings where biomass burning results in increased aerosol particulates (Ben-Ze'ev et al., 2006; Miura et al., 1998) and in regions with high pollution (Tariq et al., 2021; Zhang et al., 2016). Aerosol interference is amplified at NFW, compared to natural settings, due to its proximity to mining operations (e.g., mine dust) and frequent forest fire haze.

EVI consists of reflectance from the near infrared (NIR), red (R) and blue (B) bands within the short-wave spectrum and is calculated using:

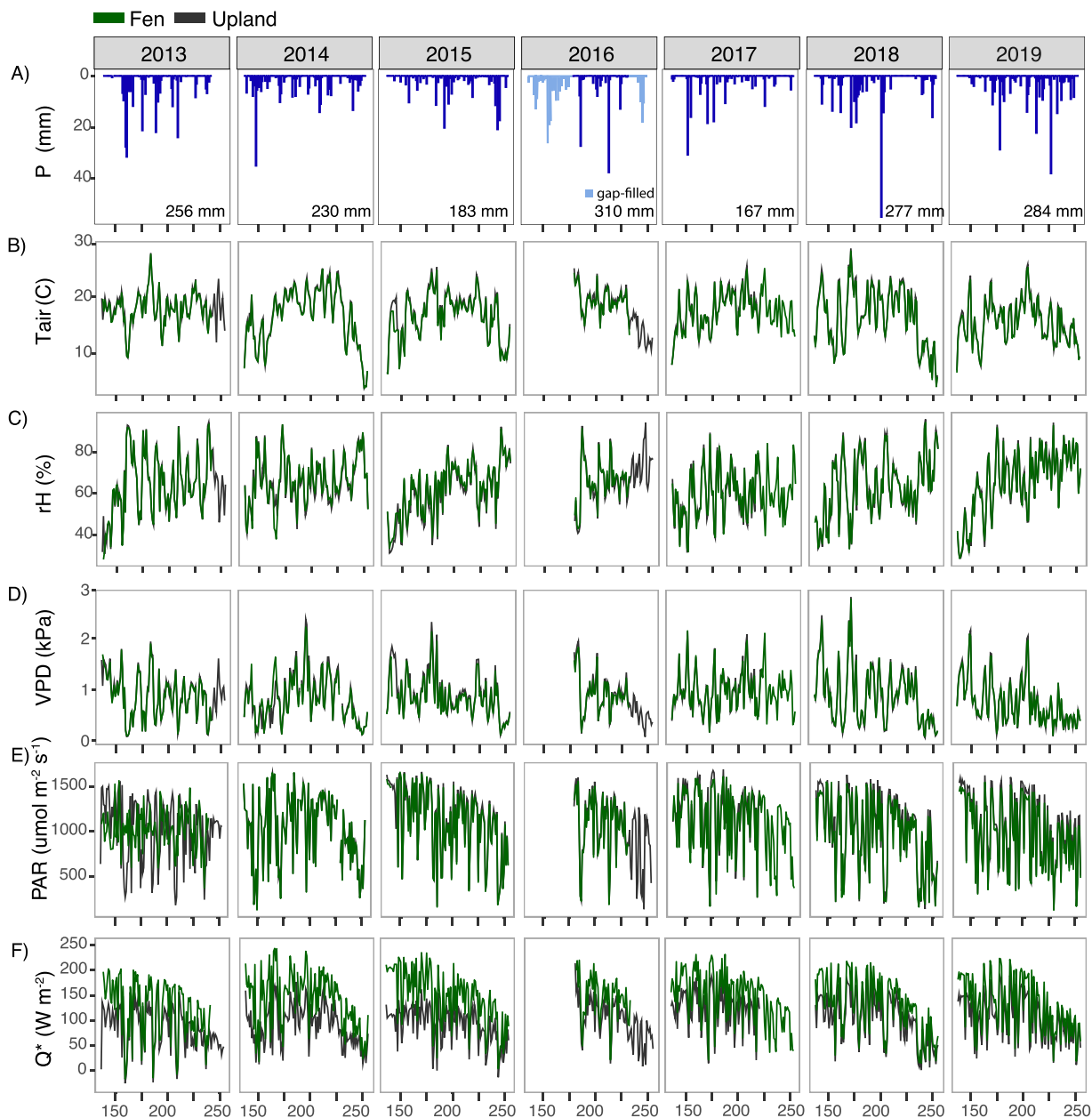


**Fig. 3.** Seven-year time series of seasonal meteorological characteristics for the Fen (green) and Upland (grey). A) Daily precipitation (P, mm). B) Mean daily air temperature ( $T_{air}$ , °C). C) Mean daily relative humidity (rH, %). D) Mean daily vapour pressure deficit (VPD, kPa). E) Mean daily mid-day (10:00 – 16:00) photosynthetically active radiation (PAR,  $\mu\text{mol m}^{-2} \text{s}^{-1}$ ). F) mean daily net radiation ( $Q^*$ ;  $\text{W m}^{-2}$ ). Note the significant overlap between fen and upland values. Due to the close proximity of the landscapes (and thus towers; <300 m apart) atmospheric conditions were largely similar. Missing data in 2016 is due to Horse Creek Wildfire. Missing data from the upland in 2017 Upland is due to instrumentation malfunction.

$$EVI = G \frac{NIR - RED}{NIR + C_1 \times RED - C_2 \times BLUE + L} \tag{1}$$

where *L* is the canopy background adjustment that addresses nonlinear, differential *NIR* and *RED* radiant transfer through a canopy, and *C1*, *C2* are the coefficients of the aerosol resistance term, which uses the blue band to correct for aerosol influences in the red band. Coefficients adopted in the EVI algorithm are, *L* = 1, *C1* = 6, *C2* = 7.5, and *G* (gain factor) = 2.5 (Huete et al., 2002, 1994; Huete et al., 1997).

Here, satellite-derived, 30-m resolution EVI provides an ecosystem scale snapshot of vegetation development using Landsat 8 imagery acquired through USGS (Vermeire et al., 2016). Temporal resolution of Landsat 8 is 8–16 days and had complete coverage during the study period. EVI was derived using the Google Earth Engine (GEE) application processing interface (API; Gorelick et al., 2017) and post-processed using a cloud masking script (modified by authors from GEE API Guides) to further remove effects of cloud cover, forest fire haze and mine dust (correcting for 75% of interference). Mean, peak-season (DoY 170–220) EVI values are presented here as a metric to spatially characterize the extent and development of vegetation in years following construction. Additionally, the mean of a 60 × 60 m pixel grid located at the epicenter of flux tower footprints was calculated to create a time series spanning 2013–2019. In order to provide context to EVI results, the grid method was applied to two nearby natural systems comprised of similar plant communities as well (saline fen and mixed wood upland).

## 4. Results

### 4.1. Environmental conditions

As the two landscapes are adjacent to one another, meteorological variables (such as *T*<sub>air</sub> and *P*) were consistent between the two landscapes. Differences between the two landscapes were most apparent in edaphic conditions and vegetation.

**Table 2**

Summary of growing season means (± SD) of NFW environmental variables: air temperature, precipitation, relative humidity, vapour pressure deficit, photosynthetically active radiation, net radiation, water table depth, soil temperature, volumetric water content (at 5, 15 and 30 cm depths), electrical conductivity (*E<sub>c</sub>*), and sodium concentration (*Na*<sup>+</sup>). *E<sub>c</sub>* and *Na*<sup>+</sup> are presented here as they depict changes in water quality during ecosystem development. Methods and a detailed analysis of solute transport and water quality changes at NFW are discussed by Kessel et al. (2018).

	<i>T</i> <sub>air</sub>	<i>P</i>	rH	VPD	PARmid-day	<i>Q</i> <sup>*</sup>	WTD	<i>T</i> <sub>soil</sub>	VWC 5 cm	VWC 15 cm	VWC 30 cm	<i>E<sub>c</sub></i> <sup>2</sup>	<i>Na</i> <sup>+2</sup>
	°C	mm	%	kPa	μmol m <sup>-2</sup> s <sup>-1</sup>	Wm <sup>-2</sup>	cm bgs	°C	%	%	%	μs cm <sup>-1</sup>	mg L <sup>-1</sup>
<b>Fen</b>													
<b>2013</b>	18 ± 5	256	64 ± 22	0.86 ± 0.71	1034 ± 620	123 ± 200	8 ± 19	16 ± 4	83 ± 3	78 ± 1	79 ± 1	2051 ± 635	96 ± 51
<b>2014</b>	17 ± 6	230	66 ± 21	0.81 ± 0.71	1091 ± 480	143 ± 212	-3 ± 1	19 ± 7	84 ± 2	75 ± 2	83 ± 2	2524 ± 832	79 ± 59
<b>2015</b>	17 ± 6	183	62 ± 22	0.85 ± 0.72	1138 ± 490	146 ± 213	11 ± 5	18 ± 7	84 ± 2	85 ± 1	89 ± 1	2606 ± 708	157 ± 89
<b>2016</b>	19 ± 5	310 <sup>a</sup>	66 ± 19	0.91 ± 0.72	1115 ± 461	147 ± 205	12 ± 5	16 ± 2	79 ± 3	84 ± 0	88 ± 1	2954 ± 1376	158 ± 99
<b>2017</b>	17 ± 6	168	60 ± 22	0.97 ± 0.77	1161 ± 459	146 ± 207	18 ± 8	16 ± 4	82 ± 5	85 ± 1	9 ± 2	2914 ± 885	179 ± 80
<b>2018</b>	17 ± 7	278	63 ± 22	0.89 ± 0.84	1006 ± 480	130 ± 189	8 ± 4	13 ± 4	85 ± 0	85 ± 1	88 ± 1	2440 ± 767	219 ± 114
<b>2019</b>	15 ± 6	285	65 ± 23	0.75 ± 0.72	1027 ± 461	130 ± 186	1 ± 6	12 ± 4	85 ± 1	85 ± 1	89 ± 1	-	112 ± 99
<b>Upland</b>													
<b>2013</b>	18 ± 5	257	64 ± 22	0.88 ± 0.73	1150 ± 476	85 ± 169	-	21 ± 7	26 ± 2	28 ± 1	38 ± 0	2623 ± 1090	269 ± 162
<b>2014</b>	17 ± 6	231	66 ± 21	0.81 ± 0.74	1109 ± 476	90 ± 168	158 ± 19	20 ± 8	21 ± 3	25 ± 3	36 ± 1	2131 ± 901	132 ± 107
<b>2015</b>	17 ± 6	183	61 ± 22	0.93 ± 0.79	1193 ± 487	91 ± 173	207 ± 7	21 ± 6	15 ± 2	17 ± 2	27 ± 2	2332 ± 812	241 ± 152
<b>2016</b>	18 ± 5	310 <sup>a</sup>	67 ± 20	0.81 ± 0.7	1044 ± 484	100 ± 181	200 ± 17	21 ± 5	16 ± 1	22 ± 1	34 ± 0	2522 ± 887	131 ± 72
<b>2017</b>	18 ± 6	141	59 ± 22	0.99 ± 0.77	1200 ± 489	124 ± 197	220 ± 10	20 ± 4	15 ± 4	19 ± 5	29 ± 6	3254 ± 1195	180 ± 66
<b>2018</b>	17 ± 7	278	63 ± 22	0.9 ± 0.85	1073 ± 511	103 ± 175	213 ± 20	19 ± 5	18 ± 5	21 ± 5	31 ± 3	2596 ± 997	184 ± 148
<b>2019</b>	16 ± 6	285	65 ± 23	0.76 ± 0.73	1106 ± 493	106 ± 176	257 ± 19	18 ± 5	22 ± 9	23 ± 5	33 ± 3	-	-

<sup>a</sup> Fen and upland 2016 *P* gap-filled due Horse River fire evacuations <sup>2</sup> Mean value from all well and piezometer depths, reported by Kessel et al. (2018).

#### 4.1.1. Climatic conditions

Tair throughout the growing seasons varied between  $-4$ – $36$  °C (Fig. 3B), while average seasonal temperatures ranged between 15.5 and 19.3 °C and were consistently above the 30-year climate normal (13.3 °C; Table 2). June, July, August (JJA) average temperatures ranged from 17.4 to 20.3 °C (again, above the 15.7 °C 30-year normal), with 2016 being the warmest and 2019 the coolest. Based on Tair and P trends, 2015 and 2017 were considered warmer, drier years ( $<200$  mm year<sup>-1</sup>), while 2018, 2019 were cooler and wetter (Table 2).

P ranged between 168 (2017) and 310 mm (2016), and all years except 2016 and 2019 had less rainfall than the 30-year average (283.4 mm; Fig. 3 A). Interannual variability in the timing, frequency and intensity of rain events was also present throughout the study period. Generally, most rainfall occurred during the months of June and July with the exception of 2019, where 126 mm (44% of seasonal rainfall) occurred in August. Over the seven-year study period, 75% of rain events were  $< 5$  mm day<sup>-1</sup>. Large/intense rain events ( $>30$  mm day<sup>-1</sup>) typically occurred towards the end of July and into August (2018, 2019). Of note is July 2018, where 86 mm of rain fell over 4 days (30% of 2018 total rainfall), resulting in extensive ponding within the fen.

Maximum photosynthetically active radiation (PAR) typically occurred in mid to late June (between DoY 155–180), ranging between 1590 and 2042  $\mu\text{mol m}^{-2} \text{s}^{-1}$ . During peak season, PAR was highest between 11h00–17h00, with an interannual average of 947  $\mu\text{mol m}^{-2} \text{s}^{-1}$ . By mid-August, PAR begins its autumn decline with daytime values averaging 731  $\mu\text{mol m}^{-2} \text{s}^{-1}$ . A wide range of daily relative humidity values with an interannual average of 64% (Fig. 3 C) was observed. Of note, was the relatively large VPD, which remained relatively constant both intra and inter seasonally and reflected a large atmospheric demand for ET. Average seasonal VPD ranged between 0.75 (2019) to 0.97 (2017) kPa, with fluctuations in seasonal variability mirroring rainfall events (lower during wet periods/years) (Fig. 3D). Interannual net radiation ( $Q^*$ ) varied between the fen (137  $\text{Wm}^{-2}$ ) and upland (99  $\text{Wm}^{-2}$ ). Fen  $Q^*$  had remained relatively constant from 2014 onwards, whereas upland  $Q^*$  exhibited an increasing trend as vegetation continued to mature. A more detailed examination of the surface energy balance is discussed in Popović et al. (in prep).

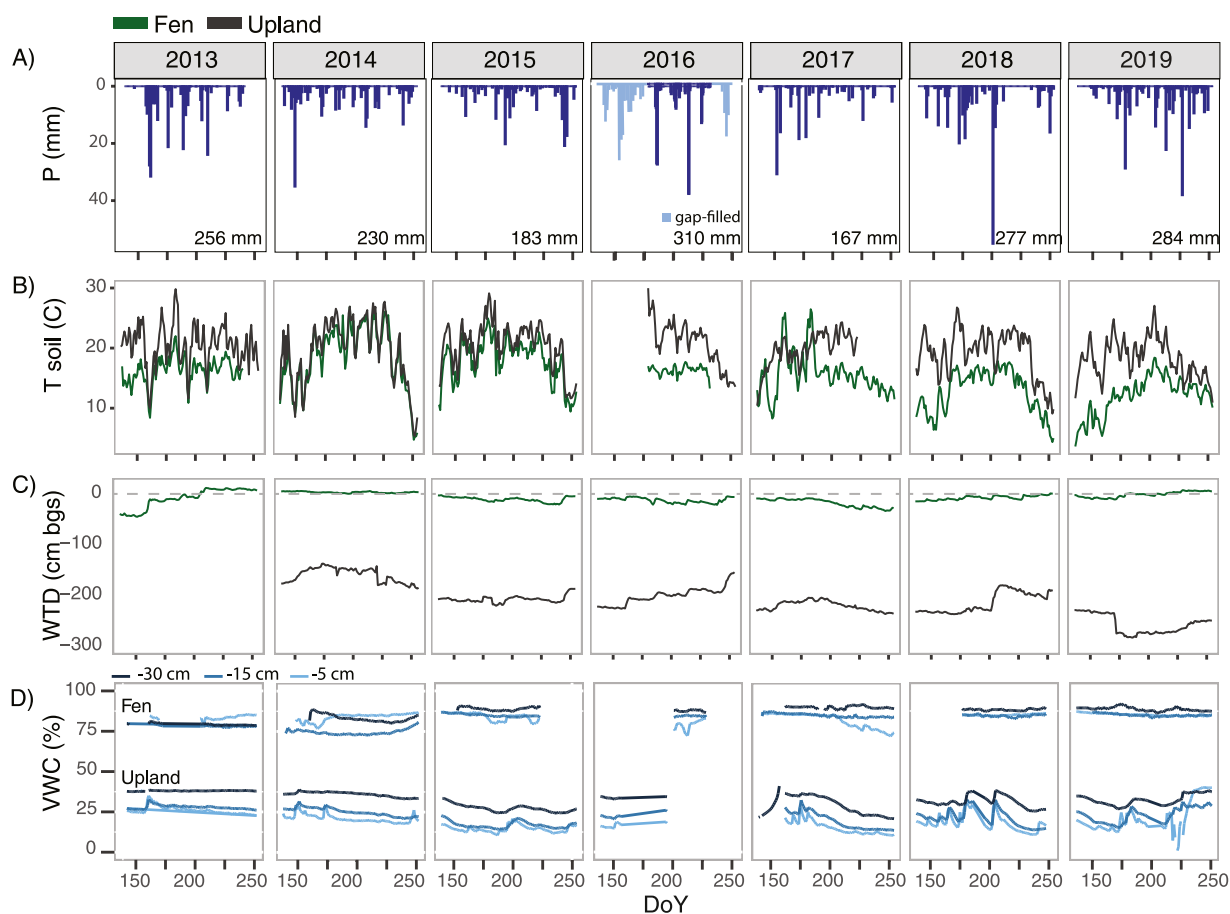


**Fig. 4.** Time series of edaphic and water table conditions in the Fen (green) and Upland (grey) from 2013 to 2019). A) Daily precipitation (mm). B) Mean daily soil temperature (C) at 5 cm below ground surface. C) Mean daily water table levels (cm below ground surface). D) soil moisture conditions (volumetric water content) at 5 (light blue), 15 (blue) and 30 (dark blue) cm below ground surface.

#### 4.1.2. Edaphic conditions

Water table (WT) position varied significantly between the two landscapes, being generally near the surface (interannual mean 8 cm bgs) in the fen and much deeper (interannual mean 209 cm bgs; Fig. 4C) in the upland. Seasonally, mean water table depth (WTD) fluctuated slightly in the fen between wetter (2014, 2018, 2019) and drier years (2015, 2017). The largest range in fen WTD was in the year following construction (2013, –13 to 45 cm bgs); however, the initially low WT was during the wetting-up period of the fen. Mean upland WTD ranged between 158 cm bgs in 2014–257 in 2019. In both landscapes, smaller scale (<10 mm), sporadic rain events appear to have a negligible impact on WTD position, however, larger or recurring rain events (2018) or prolonged dry periods (2017) influenced WTD (Fig. 4A, C).

Edaphic conditions between the two landscapes varied significantly due to differences in substrate that affect the soil water holding capacity and the aforementioned differences in WTD. Fen soil temperatures varied from –4 (Sept 2014) to 29 °C (June 2015) (Fig. 4B). Seasonally, mean peat temperatures decreased over time from  $16.6 \pm 4$  (2013) to  $12.1 \pm 4$  °C (2019). Warmest mean seasonal peat temperatures occurred in 2014 ( $18.6 \pm 7$  °C). Mean seasonal upland soil temperature varied less across all years, decreasing only slightly over time from  $20.5 \pm 7$  (2013) to  $18.3 \pm 5$  °C (2019).

Soil volumetric water content (VWC) was measured at 5, 15, and 30 cm bgs. In both landscapes, 30 cm values were consistently wettest (87% fen, 33% upland) and upper 5 cm driest (83% fen, 19% upland) (Fig. 4D). Fen VWC remained high throughout all years, ranging between 72% and 92% (Fig. 4D). Moreover, fen VWC appeared to remain relatively stable, with only slight increases occurring during large rain events. However, prolonged dry periods in the fen led to a decline in moisture content in the near surface (top 5 cm), as exhibited in 2017 when values dropped from 85% down to 72% (Fig. 4D). During wetter years, fen VWC measured at 15 cm depth was 2–6% drier than the upper, near surface peat, while the opposite trend emerged during drier years (5 cm typically drier than deeper peat). Upland soil layers exhibited larger differences between depths and were generally much drier. Mean daily VWC ranged from 10% to 40% (Fig. 4D). In contrast to the fen, upland VWC showed rapid responses to rain events, resulting in values fluctuating up to 20% over a few days (see years 2018, 2019 in Fig. 4D).

**Table 3**

Summary of average ( $\pm$  SD) vegetation biometrics for the NFW fen and upland from 2013 to 2019 including seasonal aboveground biomass (measured in the fen only), leaf area index (LAI), enhanced vegetation index (EVI) for the growing season and peak season (DoY 170 – 220), vegetation or tree height, diameter at breast height (dbh) and litter thickness. – represents years where measurement was unavailable due to juvenile plant size (fen 2013; upland 2013–2016) and/or incomplete data due to instrument malfunctions or unfavourable environmental conditions.

	AbovegroundBiomass <sup>a</sup>	LAI	EVI	EVI	Vegetation Heightcm			Litter Thickness
	g m <sup>-2</sup>		growing season	peak season	Carex	Juncus	Typha	cm
<b>Fen</b>								
2013	–	–	0.18 $\pm$ 0.04	0.21 $\pm$ 0.03	–	–	–	–
2014	395 $\pm$ 46	0.4 $\pm$ 0.14	0.24 $\pm$ 0.06	0.26 $\pm$ 0.03	8.6 $\pm$ 5.0	8.2 $\pm$ 2.8	–	–
2015	518 $\pm$ 29	1.21 $\pm$ 0.08	0.36 $\pm$ 0.11	0.44 $\pm$ 0.01	–	–	–	2.7 $\pm$ 1.6
2016	557 $\pm$ 38	–	0.45 $\pm$ 0.12	0.49 $\pm$ 0.07	–	–	–	–
2017	521 $\pm$ 34	1.77 $\pm$ 0.18	0.47 $\pm$ 0.16	0.57 $\pm$ 0.06	51.3 $\pm$ 10	45.5 $\pm$ 5	95 $\pm$ 26	12 $\pm$ 6.2
2018	412 $\pm$ 38	0.59 $\pm$ 0.07	0.38 $\pm$ 0.14	0.49 $\pm$ 0.03	46 $\pm$ 7	47 $\pm$ 9	101 $\pm$ 28	16.2 $\pm$ 7.6
2019	442 $\pm$ 31	1.63 $\pm$ 0.26	0.32 $\pm$ 0.09	0.39 $\pm$ 0.02	54 $\pm$ 14	41 $\pm$ 12	105 $\pm$ 23	17.8 $\pm$ 9.5
					<b>Deciduous</b>		<b>Coniferous</b>	
					height (m)	dbh (cm)	height (m)	dbh (cm)
<b>Upland</b>								
2013	–	–	0.16 $\pm$ 0.03	0.17 $\pm$ 0.02	–	–	–	–
2014	–	–	0.21 $\pm$ 0.03	0.23 $\pm$ 0.02	–	–	–	–
2015	–	0.62 $\pm$ 0.07	0.23 $\pm$ 0.03	0.22 $\pm$ 0.03	–	–	–	< 1
2016	–	0.79 $\pm$ 0.12	0.31 $\pm$ 0.04	0.31 $\pm$ 0.03	–	–	–	< 1
2017	–	0.82 $\pm$ 0.30	0.35 $\pm$ 0.09	0.42 $\pm$ 0.04	1.17 $\pm$ 68	1.67 $\pm$ 0.44	–	2.7 $\pm$ 0.30
2018	–	0.75 $\pm$ 0.02	0.34 $\pm$ 0.14	0.44 $\pm$ 0.05	1.70 $\pm$ 0.61	2.12 $\pm$ 0.67	1.47 $\pm$ 0.40	1.3 $\pm$ 0.58
2019	–	2.57 $\pm$ 0.20	0.41 $\pm$ 0.09	0.47 $\pm$ 0.01	1.85 $\pm$ 0.45	4.46 $\pm$ 1.2	1.58 $\pm$ 0.38	1.35 $\pm$ 0.25

<sup>a</sup> Collected and analyzed by Messner (2019)

### 4.1.3. Vegetation dynamics

Fen plant community was dominated by *Carex aquatilis*, with smaller regions of *Typha latifolia* and *Juncus balticus*, with *Typha latifolia* dominating ponded regions. The greatest increase in fen plant foliage occurred from 2014 to 2015, with aboveground biomass and LAI increasing from  $395.38 \pm 46 \text{ g m}^{-2}$  and  $0.4 \pm 0.14$ – $518.20 \pm 29 \text{ g m}^{-2}$  and  $1.21 \pm 0.08$ , respectively (Table 3; Messner, 2019). 2015 onwards, LAI remained relatively constant (interannual mean of  $1.53 \pm 0.21$ ) and values were typically largest in August. 2018 exhibited lowest foliage yields out of all developed years (aboveground biomass:  $412.14 \pm 38$ , LAI:  $0.59 \pm 0.07$ ). As of 2019, mean plant height was 54 cm (*Carex aquatilis*), 105 cm (*Typha latifolia*) and 41 cm (*Juncus balticus*). *Carex aquatilis* and *Typha latifolia* both produce large amounts of seasonal litter, resulting in litter thickness at the fen varying between 5 and 27 cm thick (18 cm average) as of 2019 (Table 3).

Upland trees developed slowly during initial years and became robust by 2017. Prior to 2017, the upland was dominated by patches of bare ground, understory vegetation (shrubs and dry grasses) and juvenile trees. Upland LAI ranged from 0.02 (2013) to 2.56 (2019; Table 3). Typically, peak LAI values were observed in July with broadleaf species senescing by mid-August. As of 2019, mean tree height of all species ranged between 1.14 and 1.87 m (Table 3). Variability in tree height and DBH was large for *Populus balsamifera* due to the significant abundance of tree saplings in the transect area (excluding saplings, average height and DBH are 1.9 m, 4.2 cm).

Seasonal mean EVI values for the fen illustrate the rapid increase from bare ground in 2013 ( $0.18 \pm 0.04$ ) to expansive plant coverage by 2015 ( $0.36 \pm 0.1$ ) (Fig. 5A), with an  $\text{EVI} > 0.2$  representing a vegetative signal (Huete et al., 2002). From 2015 onwards, mean seasonal EVI fluctuated between  $0.32 \pm 0.09$  (2019) to  $0.47 \pm 0.16$  (2017). Mean peak season EVI values varied between early years (2013–2014) and later years (2015–2019), after vegetation became established, from 0.25 to 0.48, respectively. 2017 exhibited the highest mean peak season EVI of  $0.59 \pm 0.06$ .

Upland EVI values increased annually, but at a slower rate, compared to the fen, with values remaining low from 2013 to 2016 (interannual mean  $0.23 \pm 0.0$ ; Fig. 5A). As trees matured, EVI increased from 2017 onwards (interannual mean  $0.44 \pm 0.02$  h; Fig. 5A; Table 3).

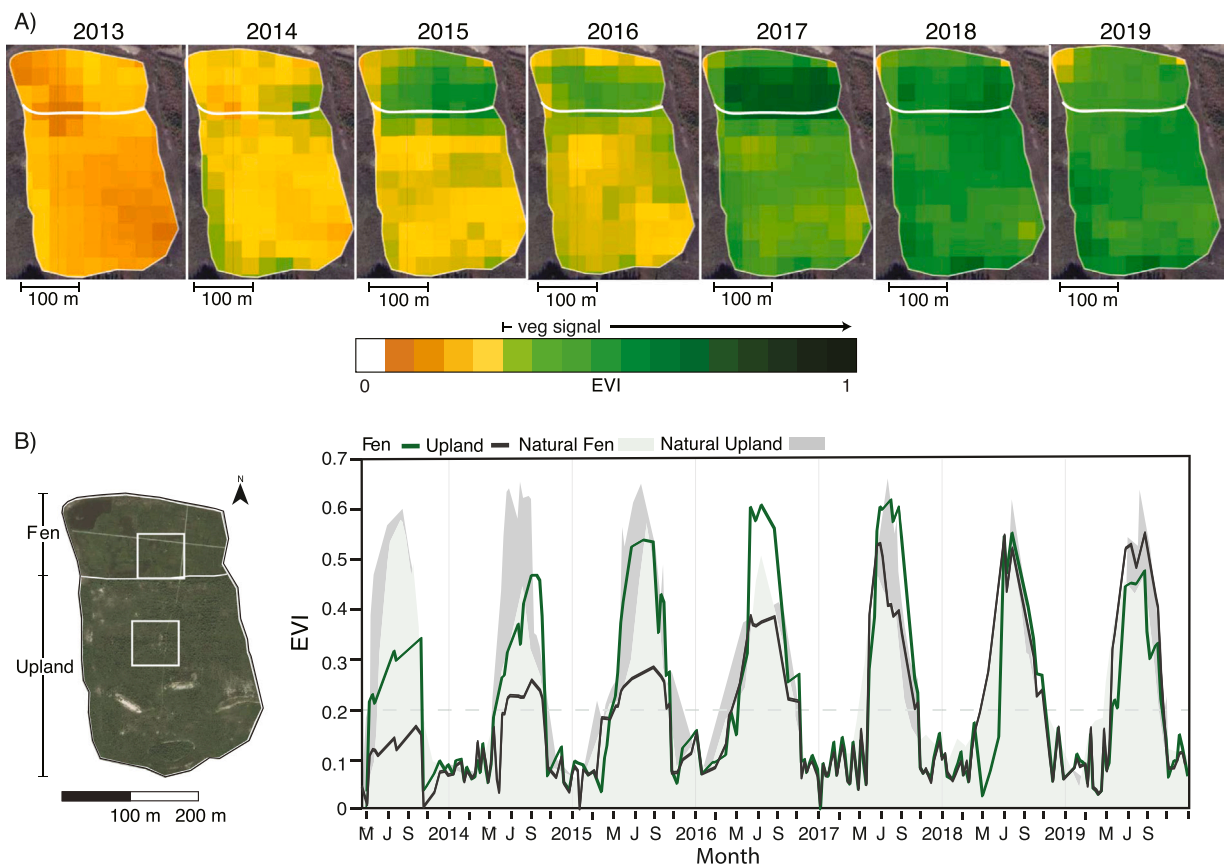


Fig. 5. Temporal snapshot of plant development in the fen and upland from 2013 to 2019. A) Ecosystem scale mean peak season (DoY 170–220) Enhanced Vegetation Index (EVI). B) Timeseries of EVI values from the mean of a pixel grid ( $60 \times 60 \text{ m}$ ) located at the epicenter of flux tower footprints (white square). Light green and grey shading depict values from nearby natural sites with similar plant compositions.

## 4.2. Carbon dynamics

### 4.2.1. Gross ecosystem production (GEP)

Total GEP in the fen increased significantly, with total growing season values of 24 g C m<sup>-2</sup> in 2013–279 g C m<sup>-2</sup> in 2019 (Table 4A). Following planting (2014 onwards), seasonal fen GEP has remained above 279 g C m<sup>-2</sup> (2019). Highest seasonal GEP occurred in 2015 at 512 g C m<sup>-2</sup>, coinciding with the first year that vegetation was robust and expansive across the entire fen. Peak season (DoY 170–220) daily average GEP ranged from 0.7 ± 0.8 g C m<sup>-2</sup> day<sup>-1</sup> (2013) to 5.6 ± 1.5 g C m<sup>-2</sup> day<sup>-1</sup> (2015) (Table 4B). Peak season interannual average daily GEP was 4.4 ± 1.3 g C m<sup>-2</sup> day<sup>-1</sup>. 2019 had the lowest peak season average at 3.4 ± 0.7 g C m<sup>-2</sup> day<sup>-1</sup> and overall lowest trends in GEP out of the years with vegetation (2014 onwards). Highest daily GEP typically occurred in July (between DoY 180–210) and ranged between 2.6 (2013) to 8.4 (2015) g C m<sup>-2</sup> day<sup>-1</sup>. Average seasonal daily GEP ranged between 0.5 ± 0.5–5.2 ± 1.6 g C m<sup>-2</sup> day<sup>-1</sup> (Table 4B).

In the upland, total seasonal GEP increased from 65 in 2013–439 g C m<sup>-2</sup> in 2019. Lowest average daily upland GEP was in 2013 at 0.5 ± 0.3 g C m<sup>-2</sup> day<sup>-1</sup>, followed by an increase in 2014 (2 ± 1.3 g C m<sup>-2</sup> day<sup>-1</sup>), likely due to emergence of sparse understory vegetation (Table 4A). Moreover, there was a substantial increase in upland daily GEP in 2018 and 2019 (3.7 ± 1.7 and 3.7 ± 1.4 g C m<sup>-2</sup> day<sup>-1</sup>; Table 4B), when tree and understory vegetation were more established. 2017 onwards, seasonal GEP begins to exhibit a typical parabolic shape that follows foliation, peak season, and senescence in deciduous tree dominated ecosystems (Fig. 6B). Similar to the fen, highest rates of GEP in the upland occurred between DoY 171 – 215, with later years all occurring before day 200 (191, 171, 181). Maximum daily GEP ranged from 1.4 (2013) to 7.9 (2018) g C m<sup>-2</sup> day<sup>-1</sup>.

### 4.2.2. Respiration (R<sub>eco</sub>)

Total seasonal fen ecosystem respiration (R<sub>eco</sub>) also fluctuated during the first three years (2013–2015) ranging between 94 g C m<sup>-2</sup> (2013) to 404 g C m<sup>-2</sup> (2014, Fig. 5A; Table 4A). From 2016 onwards, total R<sub>eco</sub> remained relatively stable, ranging between 102 and 268 g C m<sup>-2</sup> seasonally (Fig. 6; Table 4A). Daily average R<sub>eco</sub> ranged between 1.3 ± 0.4–3.4 ± 1.6, 2 g C m<sup>-2</sup> day<sup>-1</sup> (Table 4B).

Overall, upland R<sub>eco</sub> was greater than in the fen across all years, with totals ranging from 207 (2016) to 620 g C m<sup>-2</sup> (2014). Lower totals in 2016 and 2017 (246, 267 g C m<sup>-2</sup>) were the result of missing data from tower malfunctions and fire evacuation. Higher R<sub>eco</sub> in the upland compared to the fen corresponds to the higher upland soil temperatures and lower soil moisture (Fig. 4).

### 4.2.3. Net ecosystem exchange (NEE)

The fen quickly developed from a carbon source (70, 2013) to a steady sink by 2015 (–243 g C m<sup>-2</sup>) after which NEE remained a relatively stable sink of CO<sub>2</sub> (Table 4A, Fig. 7). Average daily NEE ranged from 1.5 ± 0.4 (2013) to – 3.3 ± 1.4 g C m<sup>-2</sup> day<sup>-1</sup> (2015), with highest NEE rates typically occurring in early July (Fig. 6). The highest daily rate of NEE occurred in 2016 at – 6.2 g C m<sup>-2</sup> day<sup>-1</sup>. Peak NEE occurred between DoY 185–206 in all years except for 2014 (DoY 243). Daily peak season uptake from 2015 to 2019 ranged between – 1 ± 1 (2019) to – 3.3 ± 1.4 (2016) g C m<sup>-2</sup> day<sup>-1</sup> (Table 4B). In 2015 the fen was a daily C sink throughout the observation period (Fig. 7). From 2017 onwards, the start of daily CO<sub>2</sub> uptake occurred later each season. The timing of when net CO<sub>2</sub> uptake

**Table 4A**

Cumulative growing season (gs) and peak season (ps: DoY 170–220) carbon and ET fluxes from the fen and upland (2013 – 2019). CO<sub>2</sub> uptake represents the number of days with CO<sub>2</sub> uptake (based off on daily NEE) over 120 growing season days.

A) Totals	NEE		R <sub>eco</sub>		GEP		CO <sub>2</sub> Uptake	ET		P-ET
	gC m <sup>-2</sup>		gC m <sup>-2</sup>		gC m <sup>-2</sup>		days	mm		mm
	gs	ps	gs	ps	gs	ps		gs	ps	
<b>Fen</b>										
2013 <sup>a</sup>	70	24	94	35	24	11	0	326	164	-70
2014	-69	-1	404	225	474	226	86	424	212	-193
2015	-244	-123	269	145	512	268	114	452	207	-268
2016 <sup>c</sup>	-179	-151	102	84	281	235	53	207	166	-87
2017	-215	-131	158	85	373	216	109	328	159	-160
2018	-186	-128	202	111	388	239	100	348	184	-71
2019	-123	-86	156	86	279	172	95	296	148	-12
<b>Upland</b>										
2013	519	208	585	240	65	32	0	243	131	14
2014	385	221	620	312	235	92	0	210	103	21
2015	398	201	514	256	117	55	0	188	94	-5
2016 <sup>c</sup>	120	73	247	151	126	78	1	147	94	-27
2017 <sup>b</sup>	73	67	267	191	194	123	21	207	118	-66
2018	134	46	579	303	445	257	17	260	140	18
2019	46	25	485	249	439	224	43	248	127	37

<sup>a</sup> Fen 2013: incomplete data due to EC tower instrument malfunction (n = 47; where n = number of days measured out of 120, see Fig. 7).

<sup>b</sup> Upland 2017 incomplete data due to EC tower instrument malfunction (n = 87)

<sup>c</sup> Fen and upland 2016 incomplete data due Horse River fire evacuations (n = 54 (fen), 79 (upland))

**Table 4B**

Daily growing season (gs) and peak season (ps) mean ( $\pm$  SD) carbon (NEE,  $R_{eco}$ , GPP) and water fluxes (ET, WUE) from 2013 to 2019.

B) Daily	NEE		$R_{eco}$		GEP		ET		WUE		
	g C m <sup>-2</sup> day <sup>-1</sup>		g C m <sup>-2</sup> day <sup>-1</sup>		g C m <sup>-2</sup> day <sup>-1</sup>		mm day <sup>-1</sup>		g C kg H <sub>2</sub> O <sup>-1</sup> day <sup>-1</sup>		
	gs	ps	gs	ps	gs	ps	gs	ps	gs	ps	
<b>Fen</b>											
2013 <sup>a</sup>	1.5 ± 0.4	1.5 ± 0.4	2 ± 0.8	2.2 ± 1	0.5 ± 0.5	0.7 ± 0.8	3.8 ± 1.8	4 ± 1.9	0.6 ± 1.0	0.6 ± 0.6	
2014	-0.6 ± 1.1	0 ± 0.9	3.4 ± 1.6	4.4 ± 1.3	4 ± 1.4	4.4 ± 1.5	3.6 ± 1.4	4.2 ± 1.2	1.5 ± 1.7	1.5 ± 0.7	
2015	-2 ± 0.8	-2.4 ± 0.8	2.3 ± 0.8	2.8 ± 0.7	4.3 ± 1.4	5.2 ± 1	3.8 ± 1.3	4.1 ± 1.3	1.8 ± 1.3	1.8 ± 0.4	
2016 <sup>c</sup>	-3.3 ± 1.4	-3.6 ± 1.4	1.9 ± 0.4	2 ± 0.3	5.2 ± 1.6	5.6 ± 1.5	3.8 ± 1.1	3.9 ± 1.2	2.1 ± 1.7	2.1 ± 0.7	
2017	-1.8 ± 1.2	-2.6 ± 1.1	1.3 ± 0.4	1.7 ± 0.3	3.1 ± 1.4	4.2 ± 1.1	2.8 ± 0.8	3.1 ± 0.9	1.7 ± 1.3	1.7 ± 0.4	
2018	-1.6 ± 1.4	-2.5 ± 1	1.7 ± 0.5	2.2 ± 0.3	3.3 ± 1.7	4.7 ± 1	2.9 ± 1.2	3.6 ± 1.2	1.8 ± 1.3	1.8 ± 0.4	
2019	-1 ± 1	-1.7 ± 0.8	1.3 ± 0.5	1.7 ± 0.5	2.3 ± 1.3	3.4 ± 0.7	2.5 ± 0.9	2.9 ± 0.9	1.5 ± 1.1	1.5 ± 0.3	
<b>Upland</b>											
2013	4.4 ± 1	4.1 ± 0.9	4.9 ± 1.1	4.7 ± 1	0.5 ± 0.3	0.6 ± 0.3	2 ± 1.1	2.6 ± 1.2	1.0 ± 0.8	1.1 ± 0.8	
2014	3.2 ± 1.4	4.3 ± 0.6	5.2 ± 1.9	6.1 ± 1.8	2 ± 1.3	1.8 ± 1.5	1.8 ± 0.7	2 ± 0.7	1.5 ± 0.8	1.2 ± 0.8	
2015	3.3 ± 1	3.9 ± 0.6	4.3 ± 1.2	5 ± 0.9	1 ± 0.5	1.1 ± 0.6	1.6 ± 0.6	1.8 ± 0.7	1.0 ± 0.4	1.0 ± 0.5	
2016 <sup>c</sup>	1 ± 0.9	1.4 ± 0.9	2.1 ± 1.7	3 ± 1.6	1.1 ± 0.9	1.5 ± 0.9	1.2 ± 1.1	1.8 ± 1	1.1 ± 0.3	1.1 ± 0.3	
2017 <sup>b</sup>	0.6 ± 1	1.3 ± 1.1	2.2 ± 1.7	3.7 ± 0.9	1.6 ± 1.5	2.4 ± 1.5	1.7 ± 1.3	2.3 ± 0.8	1.3 ± 0.6	1.4 ± 0.7	
2018	1.1 ± 0.8	0.9 ± 0.9	4.9 ± 1.4	5.9 ± 1	3.7 ± 1.7	5 ± 1.3	2.2 ± 1	2.7 ± 0.9	2.2 ± 0.5	2.3 ± 0.5	
2019	0.4 ± 0.9	0.5 ± 1	4.1 ± 1.6	4.9 ± 1.5	3.7 ± 1.4	4.4 ± 1.3	2.1 ± 0.7	2.5 ± 0.8	2.3 ± 0.7	2.2 ± 0.8	

<sup>a</sup> Fen 2013: incomplete data due to EC tower instrument malfunction (n = 47; where n = number of days measured out of 120, see Fig. 7)

<sup>b</sup> Upland 2017 incomplete data due to EC tower instrument malfunction (n = 87)

<sup>c</sup> Fen and upland 2016 incomplete data due to Horse River fire evacuations (n = 54 (fen), 79 (upland))

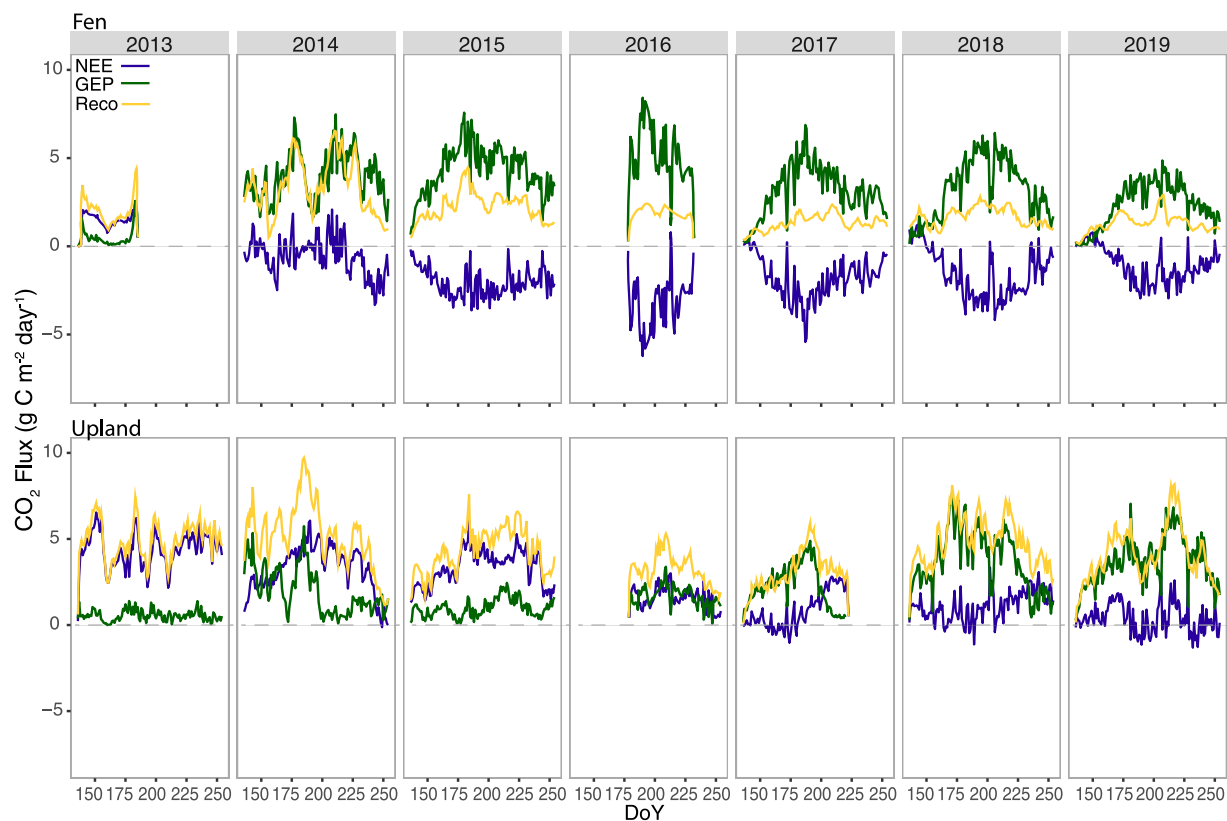


**Fig. 6.** Seven-year time series of gap-filled mean daily gross primary productivity (GEP, green), respiration ( $R_{eco}$ , red) and net ecosystem exchange (NEE, blue) for the fen (top) and upland (bottom). Negative NEE values indicate carbon uptake from atmosphere.

became prominent at the site followed plant green-up, with the latest date (post-2015) occurring in mid-June (DoY 160) in 2019.

In the upland, as vegetation became more established and GEP increased, a notable improvement in C sink capacity and daily C uptake occurred. Highest upland C emissions occurred during 2013, with 519 g C m<sup>-2</sup> released. This subsequently decreased to an

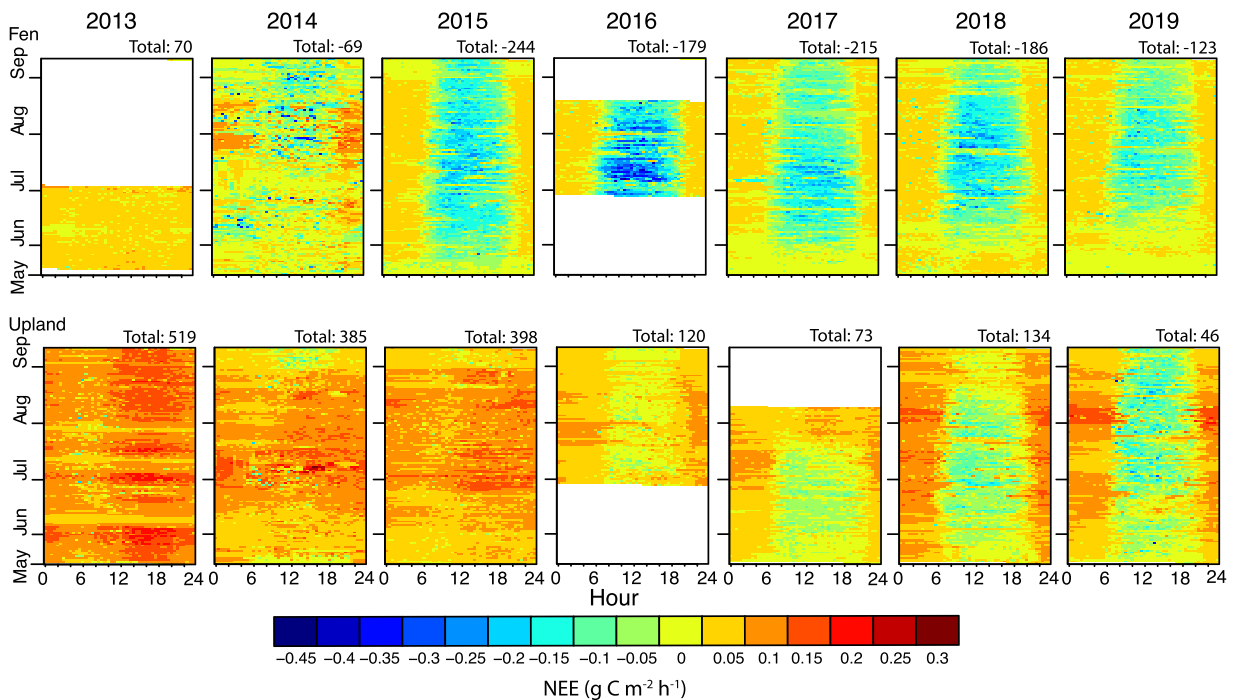


**Fig. 7.** Gap-filled half-hourly net ecosystem exchange (NEE) fluxes from 2013 to 2019 for the fen (top) and upland (bottom). Each square is a half-hourly measurement, each row a full day. Fingerprint plots show seasonal (May–Sept, y-axis) and diurnal (hourly, x axis) trends. Note clear diurnal trends of C uptake once vegetation becomes established (2015 Fen, 2017 Upland). 2016 missing data is due to Horse Creek Wildfire. 2013 Fen: July–Aug and 2017 Upland: August missing data is due to instrumentation malfunction. Positive values indicate a source of carbon to the atmosphere, negative values indicate carbon uptake by the surface.

annual source of only 46 g C m<sup>-2</sup> in 2019 (Fig. 7, Table 4A). Average daily seasonal rates decreased from 4.4 ± 1.0 g C m<sup>-2</sup> day<sup>-1</sup> in 2013–0.4 ± 0.9 g C m<sup>-2</sup> day<sup>-1</sup> in 2019 (Table 4B). From 2017 onward, daily C uptake begins to occur more frequently throughout the season (Fig. 7) from 0 days of uptake (2013–2016) to 21 days in 2017 (–8 g C m<sup>-2</sup> sequestered) and 44 days in 2019 (–22 g C m<sup>-2</sup> sequestered), equivalent to 0%, 17% and 37% of growing season days with carbon uptake, respectively.

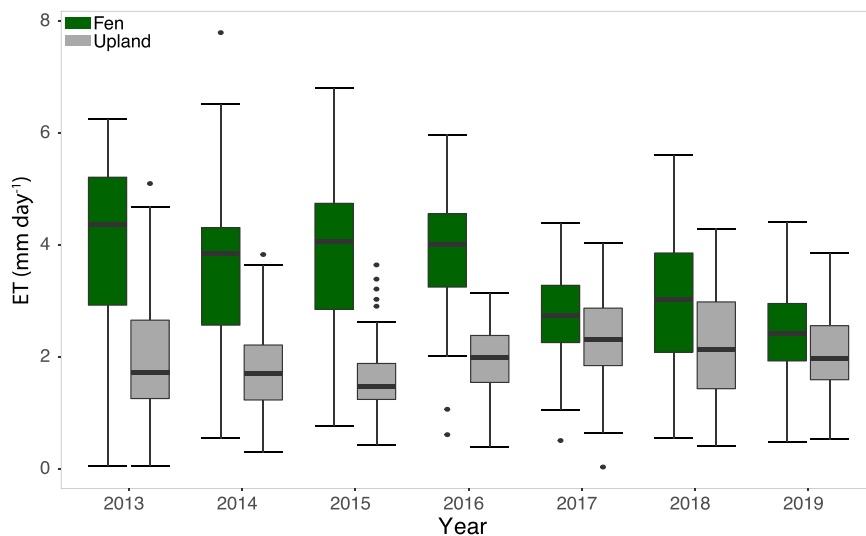


**Fig. 8.** Daily evapotranspiration (ET) rates for the fen (green) and upland (grey). Black line indicates the median ET rate, the box represents the 25th to 75th quartile, the whiskers include 95% of the range, and the black circles are outliers.

### 4.3. Water dynamics

#### 4.3.1. Evapotranspiration (ET)

Fen ET rates were higher in early years (2013–2015), in contrast to later years (2017 – 2019; Fig. 8; Table 4B). Highest daily rates typically occurred between DoY 171 – 207 (slightly earlier than peak GEP), with the highest daily ET occurring in 2014 (7.8 mm day<sup>-1</sup>, DoY 185). In later years, once vegetation growth had ensued, maximum daily ET ranged between 4.4 and 5.9 mm day<sup>-1</sup>. Fen total seasonal ET exceed precipitation in all years during the study period (Table 4A).

Upland ET had remained relatively constant, with only a slight increase from 2014 to 2019. Mean daily ET rates ranged from 1.2 ± 1.1 mm day<sup>-1</sup> (2016) to 2.2 ± 0.9 mm day<sup>-1</sup> (2018). Total seasonal ET remained relatively stable from 2013 to 2019 ranging between 147 and 260 mm (Table 4A) and exhibited a slight increase from 2017 onwards, coinciding with more mature vegetation. Upland ET exceeded seasonal precipitation in years 2015, 2016, and 2017 (Table 4A).

#### 4.3.2. Water-use efficiency (WUE)

Fen WUE increased from 0.6 ± 1.0 in year 1 (2013) to 1.5 ± 1.65 (2014) g C kg H<sub>2</sub>O<sup>-1</sup> day<sup>-1</sup> in the first full growing season (Table 4B). This was followed by a relative stabilization in WUE across later (vegetated) years (2015 onwards) with an interannual mean of 1.7 ± 0.5 (Fig. 9, Table 4B). Following the development of vegetation, even in drier years (2015, 2017) WUE rates remained relatively stable. Upland WUE has been steadily increasing as vegetation continues to mature from 1.0 ± 0.8 (2013) to 2.3 ± 0.74 (2019) g C kg H<sub>2</sub>O<sup>-1</sup> day<sup>-1</sup>.

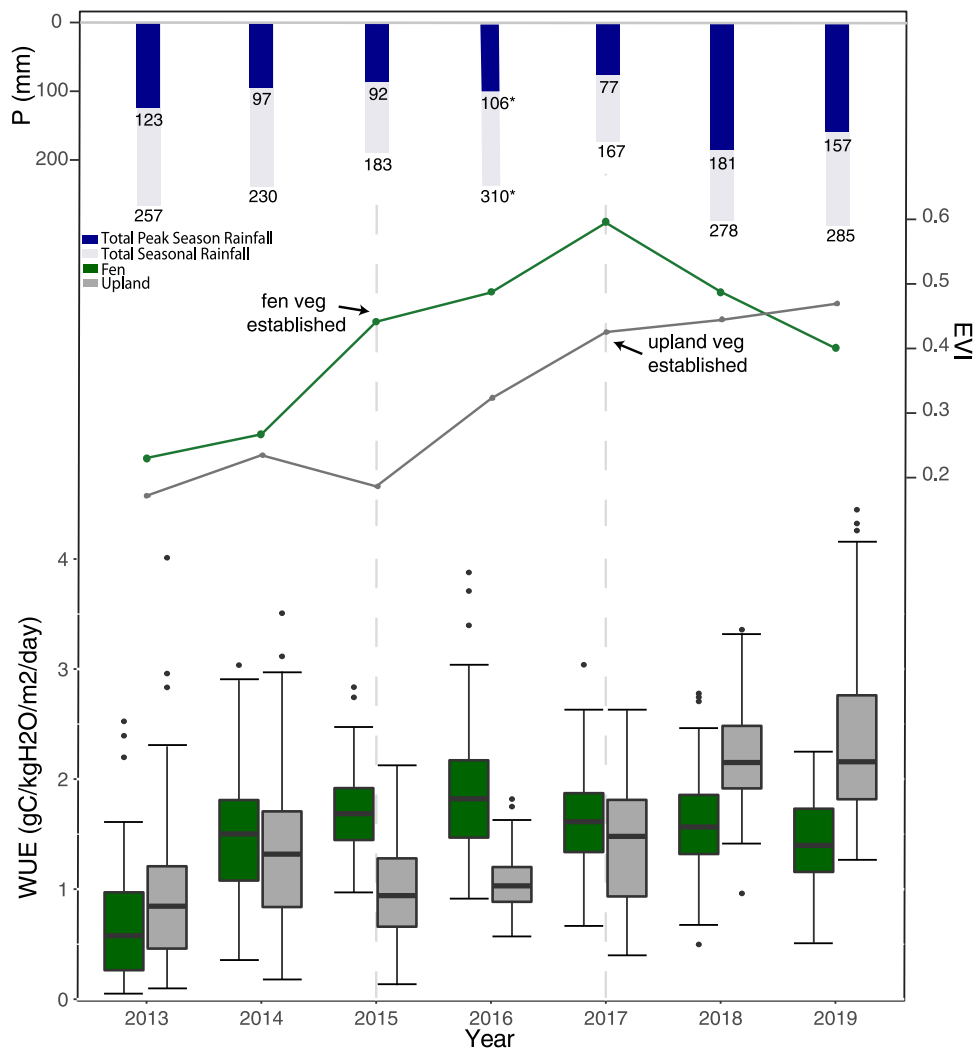


Fig. 9. Daily water use efficiency (WUE, bottom) compared to peak season EVI (middle) and growing season rainfall(top). Black line indicates the median WUE, the box represents the 25th to 75th quartile, the whiskers include 95% of the range, and the black circles are outliers.

## 5. Discussion

### 5.1. Ecosystem performance of NFW

The overarching goal of reclamation in the region is to create functional, self-sustaining, resilient ecosystems. As there is no singular metric or definition for ecosystem function, benchmarks encompassing ecologic, hydrologic and industry perspectives of ecosystem performance have been defined for NFW (Daly et al., 2012). Here, successful reclamation requires an ecosystem to be: (1) capable of supporting a representative assemblage of species; (2) carbon accumulating; and (3) able to withstand periodic environmental stress.

#### 5.1.1. Capacity for supporting representative species assemblage

Plants play a fundamental role in nutrient, carbon and water cycling as the central conduit between surface-atmosphere exchanges driven by climatic and hydrological conditions (Brümmer et al., 2012; Limpens et al., 2008; Bubier et al., 2003). Particularly in peatlands, plant community composition and species-specific phenologies control carbon uptake through plant productivity (Peichl et al., 2018) and quality of litter deposited, ultimately affecting rates of peat formation (Trites and Bayley, 2009). Specific to reclaimed AOSR landscapes, planting prescriptions must ensure efficient water use and ability to function under the expected range of environmental (i.e., saline) conditions during ecosystem evolution.

In the fen, both vascular and bryophyte species were introduced through a number of planting treatments (see Borkenhagen and Cooper, 2019). By year 3 (2015) fen vascular vegetation was widespread and robust, consisting predominantly of *Carex aquatilis* and to lesser extents *Juncus balticus*, *Typha latifolia*, *Calamagrostis inexpansa* and *Triglochin martima*. A similar rapid expansion of sedge species has also been observed at a nearby reclaimed fen (Sandhill Fen (SFW); Clark, 2018, Vitt et al., 2016) and several post-disturbance fen landscapes in Alberta, including restored seismic lines (Davidson et al., 2021) and well pads (Lemmer et al., 2020). Bryophyte establishment following moss-transfer did occur at NFW, but at a much lesser rate than expected, likely due to the rapid expansion of sedge species. Due to its tolerance of saline conditions, *Ptychostomum pseudotriquetrum* has become the dominant bryophyte species occurring throughout NFW fen, although other bryophyte species (*Calliergon giganteum*, *Campylopusium stellatum*, *Drepanocladus aduncus*, *Drepanocladus polygamus*, *Leptobryum pyriforme*) are also present (Borkenhagen and Cooper, 2019). Similar to nearby natural saline fens (Volik et al., 2018) and Sandhill Fen Watershed (Hartsock et al., 2021; Vitt et al., 2016), the spatial extent of plant assemblages at NFW-fen was driven largely by water table position and salinity. As observed in other restored and reclaimed peatland landscapes (Poulin et al., 2013; Vitt et al., 2016), *Typha latifolia* colonized most of the ponded, standing water regions of the fen. Widespread establishment of invasive *T. latifolia* may be problematic for reclamation performance, as it decays quickly and is not a peat-forming species, which may affect long term peatland function (Borkenhagen and Cooper, 2019; Trites and Bayley, 2009; Shih and Finkelstein, 2008).

Between 2014 and 2019, fen plant assemblages evolved, coinciding with changes in soil and water salinity. Fresh-water sedge and grass species in the fen such as *Carex aurea*, *Carex disperma* and *Hierochloa hitra* peaked in 2015, but were then rare or absent following increased levels of mobile sodium (Borkenhagen and Cooper, 2019). Species with a larger range of salt tolerance, such as *Juncus balticus*, *Calamagrostis inexpansa* and *Triglochin martima*, persisted and even expanded in some plots with increased salinity. In 2018, the fen experienced the highest in-flux of sodium during the study period (Table 2; Kessel et al., 2018; Sutton, 2021), resulting in visible salt-stress in *Carex aquatilis* and *Typha latifolia* (observed yellowing in foliage) and early senescence of some plots. In recent years, clusters of *Betula pumila* and *Salix pedicellaris* have developed in persistently drier regions of the fen. Overall, the fen plant community at NFW was representative of natural (saline) fens in the region (Volik et al., 2018; Purdy et al., 2005; Chee and Vitt, 1989) however, plant succession and trajectory towards herbaceous or more marsh-like vegetation may occur and could have implications on long term carbon dynamics for this site in the future.

Evolution of upland vegetation occurred at a much slower rate than the fen. Use of salvaged forest floor materials as a capping layer is common practice in forest reclamation efforts in the region (Rowland et al., 2009; Prentice, 2020; Irving, 2020) as it supports soil water retention necessary for plant growth (Sutton and Price, 2020a) and provides propagules of species common to natural boreal forests (Pinno and Hawkes, 2015; MacKenzie and Quideau, 2010). Early successional upland species at NFW were markedly different than that of other naturally regenerating forests (e.g., post-fire, post-harvest) due to dry conditions and hydrochemistry. However, similar to other reclaimed uplands (Strilesky et al., 2017; MacKenzie and Quideau, 2010; Rowland et al., 2009), the initial 5 years following construction, NFW upland consisted of a patchy understory comprising invasive forbs and grasses (*Sonchus arvensis* and *Agropyron tracycaulum*) and dry, bare ground. Although counter intuitive, these non-native, early successional species were critical to the emergence and development of planted tree species. They facilitated improved soil structure through rhizosphere development as well as litter layer establishment, which resulted in the addition of labile organic matter and nutrients (Padilla et al., 2009; Gómez-Aparicio et al., 2004; Maestre et al., 2001). Trees became prominent by year 5 (2017) and consisted of both broadleaf (*Populus tremuloides*, *Populus balsamifera*) and coniferous (*Picea mariana*, *Pinus banksiana*) species native to the region. As of 2019, the understory consisted of shrubs, graminoids, and forbs, and trees were becoming the dominant vegetation type. Notably, *Populus tremuloides* was never planted in the upland, however wind-blown seeds were likely dispersed from the nearby previously reclaimed slopes. Growth and timing of development of NFW upland tree species was similar to that of other reclaimed uplands in the region (Strilesky et al., 2017).

Remote sensing has been increasingly applied to peatland and post-disturbance studies as a means to identify plant community development and succession following disturbance (Chasmer et al., 2020; Lees et al., 2018). In this study, the derivation of remotely sensed EVI provided a more complete temporal and spatial record of plant emergence and development than fields methods alone. Once plant communities were established, EVI values measured at NFW were comparable to that of surrounding natural sites (Fig. 5)

and on par with other post-disturbance landscapes (e.g., restored peatland; Nugent et al., 2018), or those composed of similar plant communities (e.g., sedge fens: Schubert et al., 2010; Helbig et al., 2019; mixed wood boreal forest: Jahan and Gan, 2011) ranging between 0.3 and 0.6 during peak season.

Although the timing of vegetative development varied between the two landscapes, planting campaigns paired with adequate edaphic conditions resulted in establishment of a diverse plant community comprising largely native species. While saline fens are uncommon, they do exist in the WBP and are within the scope of acceptable reclamation targets (Province of Alberta, 2020). Due to the specific, altered hydrochemical and physical state of the substrate materials used in reclamation (e.g., unstratified, compressed or dried peat, presence of naphthenic acids/mobile sodium in tailing sand; Nicholls et al., 2016; Nwaishi et al., 2015b; Kessel et al., 2018; Biagi et al., 2021), plant succession and system evolution may take on a transformed, novel trajectory from the pre-disturbance landscape (Nwaishi et al., 2015a). Assigning common landscape classification to these novel ecosystems is less relevant in reclamation, and of greater importance is the functionality of plant assemblages under present and future environmental conditions.

### 5.1.2. Carbon accumulation

One of the key ecosystem functions performed by peatlands is net uptake of atmospheric CO<sub>2</sub> via photosynthesis, and the long-term storage of carbon as organic matter in peat and litter (Vasander and Kettunen, 2006; Blodau, 2002; Gorham, 1991). As NEE is typically the largest component of northern peatland annual carbon budgets (Limpens et al., 2008; Nilsson et al., 2008; Roulet et al., 2007) it was used here as a metric to quantify NFW's annual carbon function. Growing season results show significant progress towards ecosystem functionality from a CO<sub>2</sub> perspective. The fen quickly evolved from a bare-ground, growing season source of CO<sub>2</sub> in 2013 to an extensively vegetated, sink by 2015 (−243 g C m<sup>−2</sup>). Moreover, from 2015 onwards, the fen has been sequestering CO<sub>2</sub> at rates comparable to nearby natural sites (see Section 5.3). While the upland was still a growing season source of CO<sub>2</sub> in 2019 (46 g C m<sup>−2</sup>), there has been an increase in plant CO<sub>2</sub> uptake that is expected to continue as the canopy continues to develop. As a result, the NFW upland is on a trajectory towards becoming a net carbon sink in the near future.

### 5.1.3. Response to periodic environmental stress

In the seven years following inception, NFW has demonstrated resilience to periodic hydrologic stress as observed during wet and dry periods, as well as during changes in water quality (e.g., migration and influx of salts).

**5.1.3.1. Resilience to hydrologic stress.** The WPB sub-humid climate presents an additional challenge to reclamation in the region with moisture deficits and decadal dry cycles (Chasmer et al., 2018; Devito et al., 2017; Bothe and Abraham, 1993). Climate change predictions for the region project an increase in both temperature and precipitation, which may further exacerbate moisture deficits (Thompson et al., 2018; Ireson et al., 2015; Devito et al., 2012). While increased precipitation will provide more water to the system, increased temperatures will likely lengthen the growing season and enhance ET. Additionally, variability in the intensity, frequency and amount of rainfall may have unknown effects on current ecohydrological feedbacks. As such, water availability and use are critical to the long-term sustainability and performance of reclaimed systems in the AOSR. In all seven years during the study period, fen ET rates exceeded precipitation, yet vegetation was able to grow, develop and uptake CO<sub>2</sub> at rates comparable to natural sites (see 5.3 below). Notably, fen WUE rates remained relatively stable (Fig. 9) from 2015 onwards even during seasons with significantly less rainfall (seasonal rainfall ranging from 168 to 285 mm season<sup>−1</sup>).

Stable WUE is indicative of a well-connected groundwater network between the upland and fen which resulted in sufficient hydrological self-regulation during times of hydrologic stress. Additionally, because fen vegetation developed significant rooting architecture (>1 m depth in places; Messner, 2019) it was able to access water even during prolonged dry periods that resulted in water table drawdown (e.g., 2017). As a result, the system had adequate plant-water availability, and plant function was not solely dependent on P inputs – ultimately increasing resilience to (future) moisture deficits. Moreover, fen WUE rates, once vegetation became established (2015–2019 average  $1.8 \pm 1.3 \text{ g C kg H}_2\text{O}^{-1} \text{ day}^{-1}$ ), were comparable to those observed at nearby natural fens (c. f. 1.7–3.0 g C kg H<sub>2</sub>O<sup>−1</sup> day<sup>−1</sup> in Volik et al., 2021). Currently, the upland is supplying the fen with adequate water for ecohydrological functioning, however it is uncertain if this will continue as the upland canopy continues to develop, requiring more water, and water deficits continue to worsen. As trees continue to mature, ET rates are expected to increase (Strilesky et al., 2017) and will likely lead to ET > P more frequently (to date, ET > P occurred only during dry years (2015,2017)). Moreover, as the canopy develops, more water is expected to be lost through evaporation of intercepted water, resulting in less direct inputs into the soil (Fettah, 2020). However, studies of boreal aspen stands during drought conditions describe an efficient redistribution of water via aspen rooting systems (Petroni et al., 2015; Brown et al., 2014), which may ensure enough water for plant function during periods of water stress in the upland. Furthermore, Sutton and Price (2020a) modelled the hydrologic effects of upland plant growth in NFW and concluded the system will likely be capable of providing sufficient groundwater to the fen and support the development and function of an upland forest. However, the system will likely be operating just within the margins of adequate water availability. Overall, the current ecohydrological functioning of NFW is capable of adapting and coping with the climatic regime of the AOSR.

**5.1.3.2. Resilience to salt stress.** Mitigating the effects of salinization from waste materials used in reclamation in the AOSR is an ongoing challenge (Biagi et al., 2019; Kessel et al., 2018; Simhayov et al., 2017). To date, fen and upland vegetation have been able to develop and persist under current concentrations of Na<sup>+</sup> and electrical conductivity values (Table 2). However, in 2018, *Carex aquatilis* and *Typha latifolia* exhibited signs of salt stress (yellow foliage, early senescence). While NEE in 2018 remained within the range of previous years and that of natural sites, there was an observable decrease (Fig. 6,7; Table 4A and B). Additionally, there was a decrease

in biomass (Messner, 2019), LAI and EVI values (Table 3). Current hydrochemical conditions of NFW are still well within the range of levels observed at natural saline sites (Volik et al., 2021, 2019; Hartsock et al., 2021; ESRD, 2015). Planting and establishment of species ranging in salt tolerance likely helped the fen continue functioning (i.e., carbon uptake) at a comparable rate to other years. However prolonged exposure to saline conditions will likely result in a shift in the plant community and a decrease in carbon uptake capacity (Volik et al., 2018). Moreover, a number of ecohydrological and biogeochemical processes (decay rates, nutrient acquisition, plant water uptake etc.) may be affected by prolonged soil and water salinity, which may ultimately affect the long-term functionality of these landscapes (Nwaishi et al., 2015a).

## 5.2. Drivers of ecosystem functionality and interannual variability

Results indicate that ecosystem function, during the initial stages of development of a constructed, reclaimed landscape, is directly linked to the establishment and growth of vegetation. However, system design and construction are critical first steps as appropriate abiotic conditions, such as substrate quality and water availability, are required to initiate vegetation growth and persistence. Studies of boreal watersheds (natural, restored and constructed) indicate that water table dynamics, nutrient availability and hydrochemistry play a critical role in determining plant community composition (Volik et al., 2020a; Borkenhagen and Cooper, 2019; Spennato et al., 2018; Vitt et al., 2016; Dieleman et al., 2015; Koropchak et al., 2012, Trites and Bayley, 2009; Eppinga et al., 2009a; Strack et al., 2006; Lavoie et al., 2005). The relatively quick initiation of a widespread and robust sedge community in the fen was likely facilitated by planting and initial growth occurring in relatively wet years (2013, 2014, Fig. 3 A), as well as the relatively quick initiation of stable, near surface water table conditions following construction (Fig. 4C). In reclaimed AOSR uplands, growth and persistence of plants is driven by available soil moisture, which is facilitated largely by cover soil composition and thickness (Sutton and Price, 2020a; Gingras-Hill et al., 2018). Spatial variability in the timing of plant emergence in the NFW upland (Fig. 5A) was linked to the heterogeneity of soil conditions (i.e., moisture and nutrient availability). Soil moisture and capping layer thickness maps created by Sutton and Price (2020a) of NFW correspond strongly to EVI imagery presented in this study (Fig. 5A), particularly during early development (2014–2016), where areas of thicker capping materials (>30 cm) and in turn higher VWC promoted earlier plant establishment and more consistent robust growth.

### 5.2.1. Interannual variability of carbon fluxes

Results from peatland restoration (Strack et al., 2014; Strack and Zuback, 2013; Samaritani et al., 2011; Waddington et al., 2010; Petrone et al., 2001) and post-disturbance afforestation efforts (Strilesky et al., 2017; Dhar et al., 2018; Petrone et al., 2015; Mkhabela et al., 2009) indicate revegetation activities greatly reduce carbon losses and can return degraded ecosystems to carbon sinks over time. In both NFW landscapes, carbon uptake improved substantially with development of vegetation (Fig. 7, Table 4). In established plant communities, seasonal variability in carbon fluxes is largely controlled by plant physiology, growing season length, PAR and meteorological conditions (Baldocchi et al., 2018; Charman et al., 2013; Brümmer et al., 2012; Barr et al., 2007; Falge et al., 2002; Law et al., 2002; Bubier et al., 1998). Examination of interannual variability in carbon fluxes in years following plant establishment (fen, 2015–2019, Fig. 6 and 7) suggests a response to environmental changes. Notably, in 2017, the fen received only 61 mm of rainfall between July – September (compared to 154 mm in 2018, and 208 mm in 2019) resulting in a decrease in water table position and VWC (Fig. 3). As such, there was a decrease in daily GEP rates (and NEE; Fig. 6A; 7 A) in 2017 during this dry period compared to wetter years (e.g., 2018 and 2019). However, it's important to note that carbon uptake continued during this time, albeit at a lesser rate, likely due to stomatal closure to limit water loss. Daily GEP rates during the 2017 dry period ( $3.6 \pm 1.4 \text{ g C m}^{-2} \text{ day}^{-1}$ ) were comparable to those of nearby (within 40 km) natural sites in the region experiencing similar meteorological conditions at the time (daily GEP between  $1.5$  and  $4.1 \text{ g C m}^{-2} \text{ day}^{-1}$ ; Volik et al., 2021). Moreover, a similar GEP decrease under warming or drying conditions has been reported in rich fens (Adkinson et al., 2011) and sedge-dominated microforms in a poor fen (Strack et al., 2006). However, other studies in open-treed fens have shown contradictory results, where GEP increased under warming or drying conditions (Flanagan et al., 2010; Cai et al., 2010). Moreover, bryophyte dominated microforms showed less response to changing conditions (Strack et al., 2006) Thus, the response of GEP in peatlands to changing environmental conditions is complex, non-linear, and likely controlled by site-specific variables (i.e., plant community and edaphic conditions) and the overall amplitude of change (Semeraro et al., 2019). Moreover, the timing and frequency of rain events produced interseasonal variability in carbon fluxes. In 2018 rainfall events were intense, but less frequent (including 28 days with no rain between DoY 206 – 234; Fig. 2, Table 2), which contrasted with 2019, where there was weekly, and, for some parts of the season, daily, smaller rainfall events. As a result, there was variability between the two years in the number of overcast days, which limited PAR and ultimately, plant productivity. As such, 2018 exhibited higher daily GEP rates than 2019 (Fig. 6) even though both years received a similar amount of total precipitation. In particular, there was a clear decrease in  $\text{CO}_2$  uptake in the afternoon hours of 2019 (Fig. 7) due to lower PAR and overcast conditions (compared to the same time of year in 2017 and 2018). Similarly, Nijp et al. (2015) examined the effects of daytime rain events on NEE during an 11-year study in northern Sweden and found that reduced light availability, due to cloud cover during rain events, reduced net ecosystem  $\text{CO}_2$  uptake on average by  $0.23$ – $0.54 \text{ g C m}^{-2} \text{ day}^{-1}$  or  $\sim 4.4\%$  decrease in GEP throughout a growing season.

Growing season length coupled with the timing of plant emergence also affects seasonal carbon fluxes (Charman et al., 2013). There was a distinct temporal trend in the timing of plant emergence throughout fen evolution. In earlier years (2015), plant emergence, green-up and subsequent carbon uptake occurred quickly (by DoY 136; Fig. 7) due to low plant competition, adequate edaphic conditions and little to no litter layer. From 2017 onwards a delay in plant emergence was observed with daily carbon uptake beginning later each year (DoY 146, 150, 160 for 2017, 2018, 2019). This delay is likely attributed to persistence of winter conditions and ice lenses (Pulliainen et al., 2017; Charman et al., 2013; Aurela et al., 2004) and accumulation of a relatively thick litter layer

(mean litter layer thickness  $12 \pm 6.2$  cm (2017) and  $17.8 \pm 9.5$  (2019; Table 3) resulting in new growth requiring more energy (and time) to emerge. Moreover, there was variability in the timing of plant emergence (and thus plant productivity and CO<sub>2</sub> sequestration) between the fen and upland (Figure 7AB - timing of NEE signal 2017–2019) due to differences in plant community composition.

5.2.2. Interannual variability in ET

NFW ET was strongly coupled to water availability and development of vegetation, as was previously noted at NFW (Scarlett et al., 2017), and related boreal studies (Brown et al., 2010; Petrone et al., 2001; Price et al., 1998; Lafleur, 1990). Early in its development (2013, 2014), the fen surface was bare and dominated by dark, wet peat and large ponded areas (Fig. 1). As a result, ET was high (326 and 424 mm growing season<sup>-1</sup>), and close to PET. Here, ET rates were largely driven by high surface evaporation (similar to those measured off a boreal pond; Petrone et al., 2007). As vegetation developed and became widespread, ponded and bare regions were

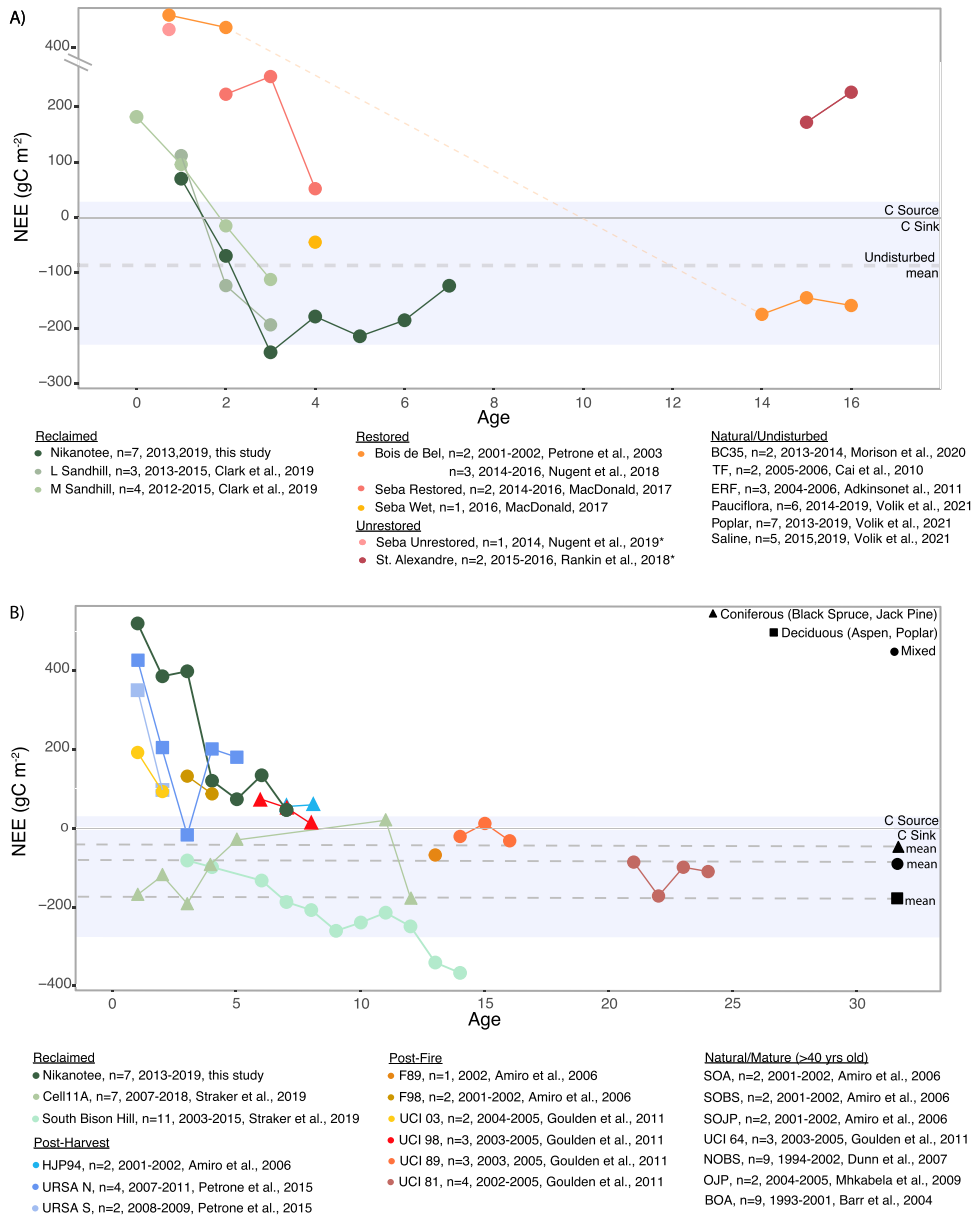


**Fig. 10.** A: Relationship between total growing season net ecosystem exchange of CO<sub>2</sub> and site age at NFW-fen compared with natural and post disturbance Canadian peatlands with eddy covariance data sets. Blue band represents the range of NEE observed at natural sites, where the small dashed line depicts mean growing season NEE of all natural sites. In the legend n is the number of study years. \* represents annual NEE. 10B: Relationship between total growing season net ecosystem exchange of CO<sub>2</sub> and site age at NFW-upland compared with mature and post disturbance (fire and harvest) boreal forests with eddy covariance data sets. Blue band represents the range of NEE observed at natural sites, small dashed line depicts mean growing season NEE of natural sites. In the legend n is the number of study years.

reduced and ET rates were subsequently driven by plant transpiration. 2015 onwards, fen ET began to decrease and stabilize as vegetation became established and fully developed (Fig. 8). Furthermore, similar to the straw mulch technique used in peatland restoration (Petroni et al., 2004; Rochefort, 2000; Price et al., 1998), development of a thick fen litter layer was likely limiting large fluctuations in surface soil temperatures and impeding surface evaporative losses (2017 onwards). The slight increase in fen ET in 2018 was attributed to the large, intense rain fall event (86 mm over 4 days; Fig. 3 A), which resulted in extensive flooding and an increase in surface evaporation. While 2018 and 2019 were both wetter years (total growing season rainfalls of 278 and 285 mm), the frequency and intensity of events differed: 2018 had less frequent, more intense events, whereas 2019 consisted of frequent, small rain events. Differences in ET trends between these two years were a clear example of how changes in intensity, timing and frequency of rainfall can impact ecohydrological dynamics. Upland ET rates increased from 2017 onwards as trees matured (five years post construction and planting (Fig. 8)). Strilesky et al. (2017) reported an increase in ET by 62% as tree cover became established within the first ten years of a nearby reclaimed forest. Amiro et al. (2006a), (2006b) describe a similar increase in ET coinciding with growth of regenerating boreal forests post wildfire.

Drivers of ecosystem functionality varied during development. Initially, abiotic factors such as soil and water chemistry, availability of water and nutrients, and adequate substrate quality, paired with climatic conditions, dictated the timing, growth, success and type of plant community development. Once a plant community became established, plant physiology and phenology drove early carbon and water fluxes. Notably, successful development of these early plant communities is likely to dictate future trajectories and overall success of the system as these early plant communities initiate and control key ecohydrological and biogeochemical feedbacks (i.e., nutrient input, litter quality, decay rate, carbon uptake) necessary for ecosystem function. Once vegetation was well established, interannual fluctuations in carbon and water fluxes were once again driven by environmental factors. Similar to natural ecosystems, NFW was able to continue functioning through interannual fluctuations in environmental conditions (see 5.1.3. Response to periodic stress). However, prolonged environmental stressors may lead to a plant successional shift (Scheffer, 2010; Eppinga et al., 2009) in the future at which point carbon and water fluxes would again be largely impacted by changes in plant form and function.

### 5.3. Comparison of NFW net ecosystem exchange rates to natural and post-disturbance landscapes

To contextualize the results and performance of NFW, NEE results were compared to natural and post-disturbance AOSR peatlands and forests. Fig. 10 summarises total growing season NEE versus age following disturbance, while providing a mean range of values recorded at natural sites (blue band). Following plant emergence (2014), the NFW fen has remained a CO<sub>2</sub> sink throughout the study period with growing season NEE ranging between -69 to -215 g C m<sup>-2</sup> (Table 4). Currently, only two upland-wetland pilot ecosystems (this study (Nikanotee Fen Watershed (NFW)) and Sandhill Fen Watershed (SFW)) have been constructed to test the design and feasibility of reclamation projects in the region. The two systems were guided by different conceptual approaches and test differing designs (Ketcheson et al., 2016). Briefly, NFW utilized numerical modelling for landscape optimization, while SFW was designed to mimic the water conserving function of natural fen systems based on their low-lying landscape position. Both systems were constructed using similar materials (i.e., by-products of the bitumen extraction process) albeit at variable thicknesses (e.g. peat thickness of 2 m at NFW vs 0.5 m at SFW) and included planting campaigns. A notable difference between the two systems is water transport and storage. In an attempt to combat the frequent periods of water stress common to the region and ensure ample inundated conditions for fen evolution, SFW was built with pumps to allow for the active management of water inputs and withdrawals, as such the system has no natural outflow for surface and near surface water (Ketcheson et al., 2016; Biagi et al., 2021). Contrastingly, there is no manual water table manipulation at NFW, fen groundwater inputs are solely supplied from the upgradient upland, and water is discharged gravitational through a natural-flowing outlet. Remarkably, these two reclaimed peatlands follow a similar (carbon) trajectory despite differences in conceptual designs and water management techniques (Clark, 2018; Ketcheson et al., 2016), likely due to the rapid initiation of plant growth immediately following construction. At both sites, the peatlands become growing season CO<sub>2</sub> sinks within 3 years following construction at uptake rates comparable to nearby natural sites (Fig. 10 A). Clark (2018) report a growing season net CO<sub>2</sub> uptake of -194 g C m<sup>-2</sup> and -112 g C m<sup>-2</sup> in the lowland and midland of SFW by year 3 (Fig. 10 A). Natural fens across the boreal exhibit a wide range of NEE values (both between sites and interannually within a single site) attributed to differences in plant community composition, edaphic conditions, and responses to hydrological dynamics and meteorological influences (Volik et al., 2021; Loisel and Yu, 2013; Charman et al., 2013; Gažović et al., 2013; Adkinson et al., 2011; Lund et al., 2010; Strack et al., 2006). A variety of natural nearby (within 40 km of NFW) fens have been concurrently monitored during the study period, including a moderately-treed poor fen (Pauciflora Fen), heavily treed moderate-rich fen (Poplar Fen) and a saline fen system (Saline Fen). Growing season NEE values for these nearby natural sites (Pauciflora, Poplar and Saline), ranged between -92 to -196 g C m<sup>-2</sup> (Pauciflora), -25 to -207 g C m<sup>-2</sup> (Poplar) and 89 to -54 g C m<sup>-2</sup> (Saline; Volik et al., 2021). Here, variability between sites is attributed largely to differences in plant community (treed with moss vs sedge) and hydrochemistry, with the saline site exhibiting lower rates of GEP due to salinity inhibiting plant productivity (Volik et al., 2021). Similarly, Morison et al. (2020) report NEE values of -25 and -130 g C m<sup>-2</sup> in a two-year study of an undisturbed, poor fen in north-central Alberta within this time frame (2013–2014). Adkinson et al. (2011) also report interannual variability in NEE in a sedge dominated, extreme rich fen in northern Alberta (-35, -154, -42 g C m<sup>-2</sup>), while NEE from a nearby moss-dominated poor fen was similar across the study period (-110.1 ± 0.5 g C m<sup>-2</sup>), further depicting the range of plant communities found in the region and their varying responses to fluctuating environmental conditions. Typically, vascular vegetation is more sensitive to environmental changes (such as WT drawdown) than mosses, due to the high water-holding capacity of moss (Kokkonen et al., 2019; Laine et al., 2021). Cai et al. (2010) measured (June – September) NEE in an Alberta treed fen over two years and reported higher values of -282 and -207 g C m<sup>-2</sup>, likely attributed to the prominent robust, mature woody vegetation. NFW-fen growing season NEE falls well within the range of values reported at natural, undisturbed sites

(Fig. 10 A).

While peatland reclamation is a novel concept, peatland restoration is not and numerous, ongoing peatland restoration endeavours provide suitable analogies of ecosystem recovery. Results from both NFW and SFW depict the importance of plant community development and emergence on ecosystem function and evolution.

Initially following construction prior to plant emergence, both NFW and SFW functioned as carbon sources (70 (NFW), 112 (SFW-lowland), 96 (SFW-midland)  $\text{g C m}^{-2}$ ). Waddington et al. (2010), measured NEE in a cutover bog in Quebec (Bois de Bel) pre- and post-restoration and reported a seasonal net  $\text{CO}_2$  loss of  $245 \text{ g C m}^{-2}$  prior to restoration. Petrone et al. (2003) reported on the first two years post-restoration of the aforementioned site, at which point  $\text{CO}_2$  emissions remained high (478 and  $468 \text{ g C m}^{-2}$ ) due to the lack of a complete cover of carbon fixing vegetation and high respiration rates from decomposing mulch. Similarly, high  $\text{CO}_2$  losses were observed during the initial year of study at adjacent restored and unrestored peatlands ( $445, 504 \text{ g C m}^{-2}$ ; Nugent et al., 2019) in northern Alberta. Furthermore, Rankin et al. (2018) reports that an unrestored peatland continues to function as a net  $\text{CO}_2$  source ( $173$  and  $259 \text{ g C m}^{-2}$ ) 15- and 16-years post-disturbance. Moreover, timing of the return to carbon sink capacity varies amongst post-disturbance sites and has been observed by year 3 in a restored cut-away peatland (Tuittila et al., 1999) and year 14 at Bois de Bel (Nugent et al., 2018). Strack and Zuback (2013) measured  $\text{CO}_2$  fluxes at Bois de Bel ten years following restoration, however, the system was still functioning as a carbon source due to WT drawdown and drier conditions resulting in increased rates of respiration. Differences in the rate and timing of carbon uptake in post-disturbance landscapes is largely driven by vegetation dynamics (i.e., vegetation emergence and establishment, plant community composition) and environmental conditions (particularly edaphic conditions, where dry conditions exacerbate respiration). Rapid emergence of wide-spread vascular vegetation, stable edaphic conditions and development of a thick litter layer resulted in GEP rates continually exceeding respiration at NFW-fen, resulting in a return to carbon sink capacity comparable to natural and restored sites. Natural (Saline fen, Volik et al., 2021) and restored (Strack and Zuback, 2013) peatlands exhibit periods of seasonal, or short-term carbon losses typically prompted by changes in water availability or hydrochemistry, which can each inhibit plant productivity. As of 2019, NFW-fen has shown resilience to environmental stressors and is expected to continue functioning (in terms of carbon uptake) like natural sites, barring any major successional shifts in vegetation.

Although there have been numerous studies assessing upland reclamation treatment materials (MacKenzie and Quideau, 2010; Naeth et al., 2013; Pinno and Hawkes, 2015) and soil structure and function (Sutton and Price, 2020b; Gingras-Hill et al., 2018; Dietrich, MacKenzie, 2018; Rowland et al., 2009), there have been limited long-term studies of carbon and water dynamics of AOSR reclaimed uplands (Straker et al., 2019; Strilesky et al., 2017). Moreover, mature stand dynamics can vary from that of juvenile or regenerating forest systems (Goulden et al., 2011). As such, here, post-disturbance (i.e., fire, harvest) regenerating boreal forests are discussed to provide context of early results and trajectory of our NFW upland. Upland WBP forests range from broadleaf leaf, aspen dominated to coniferous forests comprised of black spruce, jack pine and tamaracks, and less frequently, mixed forest comprised of both tree types. Forest type is a key driver of carbon dynamics as broadleaf forests typically have higher leaf area, GEP and ultimately  $\text{CO}_2$  uptake than coniferous species (Brümmer et al., 2012). Of the seven mature (<40 years old) forests summarised in Fig. 10B, broad leaf forests had the highest mean growing season uptake ( $-182 \pm 104 \text{ g C m}^{-2}$ ), followed by mixed tree stands ( $-73 \pm 57 \text{ g C m}^{-2}$ ) and coniferous stands ( $-7 \pm 40 \text{ g C m}^{-2}$ ; Fig. 10B). As of 2019 (year 7), NFW upland was still a source of  $\text{CO}_2$ , emitting  $46 \text{ g C m}^{-2}$ . However, it is on a trajectory to becoming a carbon sink in the next 3–5 years, which is on par with the assessments of carbon dynamics in regenerating forests. For example, Amiro et al., (2010, 2006a) examined a number of mature, post-harvest and post-fire forests across boreal regions of North America and reported that most sites became carbon sinks ten years following disturbance. Goulden et al. (2011) examined  $\text{CO}_2$  exchanges in stands ranging in age from 1 to 154 years post disturbance and found a similar temporal trend where 1- to 6-year-old sites were losing carbon (emitting between  $11$  and  $192 \text{ g C m}^{-2}$ ), 15 year old sites were beginning to gain carbon ( $-21$  to  $-32 \text{ g C m}^{-2}$  sequestered) and any sites over 25 were sequestering carbon ( $-40$  to  $-110 \text{ g C m}^{-2}$ ) at rates comparable to mature, natural sites. The lag in carbon sequestration rates in juvenile forests is attributed to the small stature and low LAI of saplings as well as respiration losses from bare forest floor. Previously reclaimed uplands in the AOSR (South Bison Hill and Cell11A on Fig. 10B) exhibited an increase in  $\text{CO}_2$  uptake almost immediately following planting, due to the emergence and rapid expansion of understory vegetation. Once trees mature, these uplands perform on par or better than mature forests (mean total seasonal NEE of  $-216 \text{ g C m}^{-2}$  for a mixed forest and  $-107 \text{ g C m}^{-2}$  for a jack pine dominated landscape; Straker et al., 2019). Similar to AOSR wetlands, forest carbon function is sensitive to environmental changes, particularly hydrologic stress. Petrone et al. (2015) examined two regenerating, aspen dominated stands and reported a return to carbon sink function by year 3 (from  $425$  to  $-17 \text{ g C m}^{-2}$  between years 1–3), followed by subsequent  $\text{CO}_2$  losses in years 4–5 ( $201$  and  $180 \text{ g C m}^{-2}$ ) due to the persistence of drought like conditions. A significant increase in tree growth and foliage in the NFW-upland from 2017 onwards resulted in a marked increase in GEP and overall  $\text{CO}_2$  uptake. However, due to the sparse understory and rather dry edaphic conditions, respiration rates remained high throughout the study period. This was in contrast to juvenile, post-fire sites, where respiration rates are typically lower in the initial years following fire as burnt soil and fire residue take longer to decompose (Czimeczik et al., 2006; Litvak et al., 2003). Nevertheless, as the canopy continues to mature, GEP is expected to increase and eventually overtake respiration as the dominant carbon flux at our upland site. Currently, the upland is following a similar trajectory to other regenerating forested systems and is expected to regain function as a carbon sink within the next 3–5 years.

## 6. Conclusions

This study captured what was likely the most dynamic period of NFW evolution, characterized by the rapid transition from a barren landscape to a flourishing ecosystem comparable to natural analogues in the region. Beginning in the first-year post-construction to the present, the system experienced rapid growth and establishment of vegetation (by 2015 in the fen, and 2017 in the upland) and

changing hydrochemical conditions. Results indicate ecosystem functionality, namely carbon and water fluxes were largely controlled by plant growth and establishment. The fen quickly evolved from a carbon source in 2013 to a stable carbon sink by 2015 (total seasonal NEE of 70 to  $-243 \text{ g C m}^{-2}$ ). The slower growth rate of trees, coupled with dry edaphic conditions in the upland, resulted in net carbon losses during the study period (NEE of  $519\text{--}46 \text{ g C m}^{-2}$  from 2013 to 2019). Similarly, WUE rates in both the fen and upland showed a marked increase once vegetation became established. Moreover, plant function and carbon uptake were able to persist throughout dry years indicating sufficient hydrological connectivity between the two landscapes and ecosystem resilience to intervals of periodic water stress. Interannual variability of fluxes suggested that plant communities are exhibiting typical responses to environmental changes, as these responses mirror those of natural sites in the surrounding area experiencing similar conditions. Barring a successional shift caused by prolonged saline or dry conditions, water and carbon fluxes of both landscapes are expected to stabilize, and future fluctuations are predicted to be controlled by meteorological influences. Assessment of  $\text{CO}_2$  and water exchanges provided sufficient evidence that the system is currently operating as intended and functioning comparably to undisturbed landscapes (fen) or post disturbance landscapes of a similar age and plant community (upland). Persistent saline conditions will likely result in a shift to more salt-tolerant species in the future which may decrease rates of plant productivity and carbon sequestration. While it is difficult to definitively predict future abiotic conditions and thus ecosystem trajectories, the fen will likely evolve towards a plant community and ecosystem functionality similar to that of fens in the region. The upland will likely be capable of supporting a forest of similar density to undisturbed sites and continue supplying adequate water to the down-gradient fen.

A limitation of this research is that NFW is a pilot project and thus the only current example of this design. As such it may not reflect the only successional path of future reclamation endeavours, particularly if designs are adjusted or baseline environmental conditions change. Thus, as future reclamation endeavours are initiated, carbon and water fluxes along with plant development should continue to be monitored to improve our knowledge base. Moreover, as the NFW is still in a juvenile phase and hydrochemistry is expected to continue changing, future work should include continued monitoring, particularly if there is a shift in plant communities. Lastly, as this study only focused on  $\text{CO}_2$  fluxes future work should include a complete carbon balance for the site to accurately assess carbon accumulation and storage.

This study is currently the longest reported record of carbon and water dynamics of a reclaimed upland-fen complex in the AOSR. Assessment of ecohydrological dynamics during early-development suggests that the constructed system is evolving towards becoming a self-sustaining, carbon-accumulating, functional ecosystem. This study demonstrates that (fen) reclamation is possible and can be successful in the AOSR. Moreover, this study applied a functional-based approach focused on a few, critical ecohydrological variables ( $\text{CO}_2$  and WUE) measured using ecosystem scale techniques (eddy covariance and remote sensing analysis). The methods used here provide a feasible approach for capturing temporal ecosystem evolution and functionality following construction and could prove useful especially for large-scale or remote reclamation endeavours where field work is not possible. This research provides a unique opportunity to assess surface-atmosphere interactions during the early successional stage of ecosystem development ultimately, improving our understanding of ecohydrological processes.

Ecohydrological insights gained from this study on the function and evolution of constructed landscapes will aid reclamation practitioners, regulatory decision-makers, and mine operators in the future design of reclamation endeavours in the region. Moreover, the rapid return of carbon sink capacity illustrated in this study paired with the ability for ecosystem functionality to persist in the water-limited setting of the AOSR may prove useful outside of the realm of reclamation as peatlands are increasingly becoming recognized as viable, nature-based solutions to climate change.

## Funding Sources

Funding for this project was provided by Natural Science and Engineering Research Council of Canada (NSERC) Collaborative Research and Development Grant to RMP and JSP (#523334), co-funded by Suncor Energy Inc., Imperial Oil Resources Ltd., and Teck Resources Ltd. and Canada First Research Excellence Fund: Global Water Futures Program and the Northern Science Training Program.

## CRediT authorship contribution statement

**Nataša Popović:** Conceptualization, Methodology, Formal analysis, Investigation, Writing – original draft, Visualization. **Richard Petrone:** Supervision, Funding acquisition, Writing – review & editing, Project administration. **Adam Green:** Software, Data curation, Writing – review & editing. **Myroslava Khomik:** Data curation, Writing – review & editing. **Jonathan Price:** Funding acquisition, Writing – review & editing.

## Declaration of Competing Interest

The authors declare that they have no known competing financial interests or personal relationships that could have appeared to influence the work reported in this paper.

## Acknowledgements

We would like to thank James Sherwood, Eric Kessel, Corey Wells, George Sutherland and all involved members of the Hydro-meteorology Research Group, Wetlands Hydrology Research Laboratory, Wetland Soils and Greenhouse Gas Exchange Lab and Reclamation Field Services at Suncor Energy for field assistance over the course of the study period. We also thank Dr. Kelly Biagi, Dr.

Scott J. Davidson and Dr. Owen Sutton, for detailed comments and discussion surrounding constructed landscapes in the AOSR. We would like to acknowledge that this research takes place within the boundaries of Treaty 8, traditional lands of the Dene and Cree, as well as the traditional lands of the Métis of northeastern Alberta. The University of Waterloo is located on the traditional territory of the Neutral, Anishnaabeg, and Haudenosaunee Peoples. The University of Waterloo is situated on the Haldimand Tract, land promised to Six Nations, which includes six miles on each side of the Grand River.

## Appendix A. Supporting information

Supplementary data associated with this article can be found in the online version at [doi:10.1016/j.ejrh.2022.101078](https://doi.org/10.1016/j.ejrh.2022.101078).

## References

- Adkinson, A.C., Syed, K.H., Flanagan, L.B., 2011. Contrasting responses of growing season ecosystem CO<sub>2</sub> exchange to variation in temperature and water table depth in two peatlands in northern Alberta, Canada. *J. Geophys. Res.: Biogeosci.* 116 (1), 1004. <https://doi.org/10.1029/2010JG001512>.
- Alberta Biodiversity Monitoring Institute (ABMI), 2017. Region overview. [Online.] Available from ([http://abmi.ca/home/reports/2018/humanfootprint/details.html?id=16#urban\\_rural](http://abmi.ca/home/reports/2018/humanfootprint/details.html?id=16#urban_rural)) [accessed 21 June 2018].
- Alberta Environment, 2008. Guideline for wetland establishment on reclaimed oil sands leases. 2nd ed. Prepared by M.L. Harris of Lorax Environmental for the Wetlands and Aquatics Subgroup of the Reclamation Working Group of the Cumulative Environmental Management Association, Fort McMurray, Alta.
- Alberta Environment and Parks (AEP), and Environment and Climate Change Canada (ECCC), 2018. Oil Sands Monitoring Program. Annual Report for 2017–2018. [Online.] Available from (<https://open.alberta.ca/dataset/dbe8811a-962e-4ce1-b2c2-ff40b8daad7a/resource/35be7d6d-083e-4d28-bf89-b92a7f3ab759/download/osm-annual-report-2017-2018-signed-by-aep-eccc.pdf>) [accessed 07 October 2019].
- Amiro, B.D., Barr, A.G., Barr, J.G., Black, T.A., Bracho, R., Brown, M., Xiao, J., 2010. Ecosystem carbon dioxide fluxes after disturbance in forests of North America. *J. Geophys. Res.: Biogeosci.* 115 (G4).
- Amiro, B.D., Barr, A.G., Black, T.A., Iwashita, H., Kljun, N., McCaughey, J.H., Saigusa, N., 2006a. Carbon, energy and water fluxes at mature and disturbed forest sites, Saskatchewan, Canada. *Agric. For. Meteorol.* 136 (3–4), 237–251. <https://doi.org/10.1016/j.agrformet.2004.11.012>.
- Amiro, B.D., Orchansky, A.L., Barr, A.G., Black, T.A., Chambers, S.D., Chapin, F.S., Randerson, J.T., 2006b. The effect of post-fire stand age on the boreal forest energy balance. *Agric. For. Meteorol.* 140 (1–4), 41–50. <https://doi.org/10.1016/j.agrformet.2006.02.014>.
- Aubinet, M., Vesala, T., Papale, D., 2012. *Eddy Covariance: A Practical Guide to Measurement and Data Analysis*. Springer.
- Aurela, M., Laurila, T., Tuovinen, J.P., 2004. The timing of snow melt controls the annual CO<sub>2</sub> balance in a subarctic fen. *Geophys. Res. Lett.* 31 (16) <https://doi.org/10.1029/2004GL020315>.
- Baldocchi, D., Chu, H., Reichstein, M., 2018. Inter-annual variability of net and gross ecosystem carbon fluxes: A review. *Agric. For. Meteorol.* 249, 520–533. <https://doi.org/10.1016/j.agrformet.2017.05.015>.
- Barr, A.G., Black, T.A., Hogg, E.H., Griffis, T.J., Morgenstern, K., Kljun, N., Nesic, Z., 2007. Climatic controls on the carbon and water balances of a boreal aspen forest, 1994–2003. *Glob. Change Biol.* 13 (3), 561–576.
- Beckingham, J.D., & Archibald, J.H., 1996. Field guide to ecosites of Northern Alberta (paperback, coil bound) (Vol. 5).
- Ben-Ze'ev, E., Karnieli, A., Agam, N., Kaufman, Y., Holben, B., 2006. Assessing vegetation condition in the presence of biomass burning smoke by applying the Aerosol-free Vegetation Index (AFRI) on MODIS images. *Int. J. Remote Sens.* 27 (15), 3203–3221.
- Biagi, Kelly M., Clark, M.G., Carey, S.K., 2021. Hydrological functioning of a constructed peatland watershed in the Athabasca oil sands region: Potential trajectories and lessons learned. *Ecol. Eng.* 166. <https://doi.org/10.1016/j.ecoleng.2021.106236>.
- Biagi, K.M., Oswald, C.J., Nicholls, E.M., Carey, S.K., 2019. Increases in salinity following a shift in hydrologic regime in a constructed wetland watershed in a post-mining oil sands landscape. *Sci. Total Environ.* 653, 1445–1457. <https://doi.org/10.1016/j.scitotenv.2018.10.341>.
- Blodau, C., 2002. Carbon cycling in peatlands: A review of processes and controls. *Environ. Rev.* 10 (2), 111–134. <https://doi.org/10.1139/a02-004>.
- Borkenhagen, A.K., Cooper, D.J., 2019. Establishing vegetation on a constructed fen in a post-mined landscape in Alberta's oil sands region: A four-year evaluation after species introduction. *Ecol. Eng.* 130, 11–22. <https://doi.org/10.1016/J.ECOLENG.2019.01.023>.
- Bothe, R.A., Abraham, C., 1993. Evaporation and evapotranspiration in Alberta, 1986–1992 Addendum. Water Resources Services. Alberta Environmental Protection: Edmonton, Canada.
- Britton, C.M., Dodd, J.D., 1976. Relationships of photosynthetically active radiation and shortwave irradiance. *Agric. Meteorol.* 17 (1), 1–7.
- Brown, S.M., Petrone, R.M., Chasmer, L., Mendoza, C., Lazerjan, M.S., Landhäusser, S.M., Devito, K.J., 2014. Atmospheric and soil moisture controls on evapotranspiration from above and within a Western Boreal Plain aspen forest. *Hydrol. Process.* 28 (15), 4449–4462. <https://doi.org/10.1002/hyp.9879>.
- Brown, S.M., Petrone, R.M., Mendoza, C., Devito, K.J., 2010. Surface vegetation controls on evapotranspiration from a sub-humid Western Boreal Plain wetland. *Process* 24, 1072–1085. <https://doi.org/10.1002/hyp.7569>.
- Brümmer, C., Black, T.A., Jassal, R.S., Grant, N.J., Spittlehouse, D.L., Chen, B., Wofsy, S.C., 2012. How climate and vegetation type influence evapotranspiration and water use efficiency in Canadian forest, peatland and grassland ecosystems. *Agric. For. Meteorol.* <https://doi.org/10.1016/j.agrformet.2011.04.008>.
- Bubier, J.L., Bhatia, G., Moore, T.R., Roulet, N.T., Lafleur, P.M., 2003. Spatial and Temporal Variability in Growing-Season Net Ecosystem Carbon Dioxide Exchange at a Large Peatland in Ontario, Canada. *Ecosystems* 6 (4), 353–367. <https://doi.org/10.1007/s10021-003-0125-0>.
- Bubier, J.L., Crill, P.M., Moore, T.R., Savage, K., Varner, R.K., 1998. Seasonal patterns and controls on net ecosystem CO<sub>2</sub> exchange in a boreal peatland complex. *Glob. Biogeochem. Cycles* 12 (4), 703–714. <https://doi.org/10.1029/98GB02426>.
- Burba, G., Schmidt, A., Scott, R.L., Nakai, T., Kathilankal, J., Fratini, G., Hanson, C., Law, B., McDermitt, D.K., Eckles, R., Furtaw, M., Velgersdyk, M., 2012. Calculating CO<sub>2</sub> and H<sub>2</sub>O eddy covariance fluxes from an enclosed gas analyzer using an instantaneous mixing ratio. *Glob. Change Biol.* 18, 385–399.
- Cai, T., Flanagan, L.B., & Syed, K.H., 2010. Warmer and drier conditions stimulate respiration more than photosynthesis in a boreal peatland ecosystem: Analysis of automatic chambers and eddy covariance measurements. <https://doi.org/10.1111/j.1365-3040.2009.02089.x>.
- Charman, D.J., Beilman, D.W., Blaauw, M., Booth, R.K., Brewer, S., Chambers, F.M., Earth, L.-D., 2013. Climate-related changes in peatland carbon accumulation during the last millennium. *Biogeosciences* 10, 929–944. <https://doi.org/10.5194/bg-10-929-2013>.
- Chasmer, L., Mahoney, C., Millard, K., Nelson, K., Peters, D., Merchant, M., Cobbaert, D., 2020. Remote sensing of boreal wetlands 2: methods for evaluating boreal wetland ecosystem state and drivers of change. *Remote Sens.* 12 (8), 1321.
- Chasmer, L.E., Devito, K.J., Hopkinson, C.D., Petrone, R.M., 2018. Remote sensing of ecosystem trajectories as a proxy indicator for watershed water balance. *Ecohydrology* 11 (7), 1–16. <https://doi.org/10.1002/eco.1987>.
- Chee, W.-L., Vitt, D.H., 1989. The vegetation, surface water chemistry and peat chemistry of moderate-rich fens in central Alberta, Canada. *Wetlands* 9 (2), 227–261. <https://doi.org/10.1007/BF03160747>.
- Chen, J.M., Cihlar, J., 1996. Retrieving leaf area index of boreal conifer forests using Landsat TM images. *Remote Sens. Environ.* 55 (2), 153–162.
- Chen, J.M., Rich, P.M., Gower, S.T., Norman, J.M., Plummer, S., 1997. Leaf area index of boreal forest: Theory, techniques, and measurements. *J. Geophys. Res.* 102 (24), 29429–29443.

- Clark, M.G., 2018, The initial biometerology of the constructed Sandhill Fen Watershed in Alberta, Canada. Retrieved from (<https://curve.carleton.ca/system/files/etd/7f6817f3-18cb-4552-93d3-5e5c447495b3/etd.pdf/25807fea42ddb6705e977037a129f980/clark-theinitialbiometerologyoftheconstructedandhill.pdf>).
- Czimecz, C.I., Trumbore, S.E., Carbone, M.S., Winston, G.C., 2006. Changing sources of soil respiration with time since fire in a boreal forest. *Glob. Change Biol.* 12 (6), 957–971. <https://doi.org/10.1111/j.1365-2486.2006.01107.x>.
- Daly, C., Price, J.S., Rezanezhad, F., Pouliot, R., Rochefort, L., Graf, M., 2012. Initiatives in oil sand reclamation: considerations for building a fen peatland in a post-mined oil sands landscape. In: Vitt, D.H., Bhatti, J. (Eds.), *Restoration and Reclamation of Boreal Ecosystems: Attaining Sustainable Development*. Cambridge University Press, Cambridge, pp. 179–201.
- Davidson, S.J., Goud, E.M., Malhotra, A., Estey, C.O., Korsah, P., & Strack, M., 2021. Linear disturbances shift boreal peatland plant communities toward earlier peak greenness. <https://doi.org/10.1002/essoar.10506838.1>.
- Davidson, S.J., Smith, M., Prystupa, E., Murray, K., Nwaishi, F.C., Petrone, R.M., Strack, M., 2021. High sulfate concentrations maintain low methane emissions at a constructed fen over the first seven years of ecosystem development. *Sci. Total Environ.* 789, 148014 <https://doi.org/10.1016/j.scitotenv.2021.148014>.
- Devito, K.J., Hokanson, K.J., Moore, P.A., Kettridge, N., Anderson, A.E., Chasmer, L., Waddington, J.M., 2017. Landscape controls on long-term runoff in subhumid heterogeneous Boreal Plains catchments. *Hydrol. Process.* 31 (15), 2737–2751. <https://doi.org/10.1002/hyp.11213>.
- Devito, K., Mendoza, C., Qualizza, C., 2012. Conceptualizing water movement in the Boreal Plains. Implications for watershed reconstruction. *Influ. Clim. Geol. Water Chem. Mov. Boreal Plain View Proj.* <https://doi.org/10.7939/R32J4H>.
- Dhar, A., Comeau, P.G., Karst, J., Pinno, B.D., Chang, S.X., Naeth, A.M., Bamphyde, C., 2018. Plant community development following reclamation of oil sands mine sites in the boreal forest: A review. *Environ. Rev.* <https://doi.org/10.1139/er-2017-0091>.
- Dieleman, C.M., Branfireun, B.A., McLaughlin, J.W., Lindo, Z., 2015. Climate change drives a shift in peatland ecosystem plant community: Implications for ecosystem function and stability. *Glob. Change Biol.* 21 (1), 388–395. <https://doi.org/10.1111/gcb.12643>.
- Dietrich, S.T., MacKenzie, M.D., 2018. Comparing spatial heterogeneity of bioavailable nutrients and soil respiration in boreal sites recovering from natural and anthropogenic disturbance. *Front. Environ. Sci.* 6, 126.
- Elmes, M.C., Price, J.S., 2019. Hydrologic function of a moderate-rich fen watershed in the Athabasca Oil Sands Region of the Western Boreal Plain, northern Alberta. *J. Hydrol.* 570, 692–704.
- Elshorbagy, A., Jutla, A., Barbour, L., Kells, J., Elshorbagy, A., Jutla, A., Kells, J., 2005. System dynamics approach to assess the sustainability of reclamation of disturbed watersheds, 1 (32), 144–158. <https://doi.org/10.1139/L04-112>.
- Environment Canada, 2015, Canadian Climate Normals 1981–2010 Station Data ([http://climate.weather.gc.ca/climate\\_normals/results\\_1981\\_2010\\_e.html?stnID=2519&autofwd=1](http://climate.weather.gc.ca/climate_normals/results_1981_2010_e.html?stnID=2519&autofwd=1)) (accessed 2.10.19).
- ESRD, Environment and Sustainable Resource Development, 2015. *Alberta Wetland Classification System*. Water Policy Branch, Policy and Planning Division,, Edmonton, AB.
- Eppinga, M.B., Max, A.E., Ae, R., Ae, M.J.W., De Ruiter, P.C., Eppinga, M.B., De Ruiter, P.C., 2009. Linking habitat modification to catastrophic shifts and vegetation patterns in bogs. *Plant Ecol.* 200, 53–68. <https://doi.org/10.1007/s11258-007-9309-6>.
- Falge, E., Baldocchi, D., Tenhunen, J., Aubinet, M., Bakwin, P., Berbigier, P., Wofsy, S., 2002. Seasonality of ecosystem respiration and gross primary production as derived from FLUXNET measurements. *Agric. For. Meteorol.* 113 (1–4), 53–74. [https://doi.org/10.1016/S0168-1923\(02\)00102-8](https://doi.org/10.1016/S0168-1923(02)00102-8).
- Fettah, S., 2020, Quantifying water use and rainfall partitioning of dominant tree species in a post-mined landscape in the Athabasca Oil Sands Region, Alberta. UWSpace. (<http://hdl.handle.net/10012/16523>).
- Foken, T., Leclerc, M.Y., 2004. Methods and limitations in validation of footprint models. *Agric. For. Meteorol.* 127 (3–4), 223–234.
- Fung, M.Y.P., Macyk, T.M., 2015. Reclamation of oil sands mining areas. *Reclamation of Drastically Disturbed Lands*. Wiley, pp. 755–774. <https://doi.org/10.2134/agronmonogr41.c30>.
- Gažovič, M., Forbrich, I., Jager, D.F., Kutzbach, L., Wille, C., Wilmking, M., 2013. Hydrology-driven ecosystem respiration determines the carbon balance of a boreal peatland ☆. *Sci. Total Environ.*, 463–464, 675–682. <https://doi.org/10.1016/j.scitotenv.2013.06.077>.
- Gingras-Hill, T., Nwaishi, F.C., Macrae, M.L., Price, J.S., Petrone, R.M., 2018. Ecological functioning of an upland undergoing reclamation on post-mining landscape of the Athabasca oil sands region, Canada. *Ecohydrology* 11 (4), e1941. <https://doi.org/10.1002/eco.1941>.
- Gómez-Aparicio, L., Zamora, R., Gómez, J.M., Hódar, J.A., Castro, J., Baraza, E., 2004. Applying plant facilitation to forest restoration: a meta-analysis of the use of shrubs as nurse plants. *Ecol. Appl.* 14 (4), 1128–1138.
- Gorelick, N., Hancher, M., Dixon, M., Ilyushchenko, S., Thau, D., Moore, R., 2017. Google Earth Engine: Planetary-scale geospatial analysis for everyone. *Remote Sens. Environ.* 202, 18–27.
- Gorham, E., 1991. Northern Peatlands: Role in the Carbon Cycle and Probable Responses to Climatic Warming. *Ecol. Appl.* 1 (2), 182–195 <https://doi.org/doi.org/10.2307/1941811>.
- Goulden, M.L., Mcmillan, A.M.S., Winston, G.C., Rocha, A.V., Manies, K.L., Harden, J.W., Bond-Lamberty, B.P., 2011. Patterns of NPP, GPP, respiration, and NEP during boreal forest succession. *Glob. Change Biol.* 17 (2), 855–871. <https://doi.org/10.1111/j.1365-2486.2010.02274.x>.
- Government of Alberta, 2017b, Facts and statistics. [Online]. Available from: (<https://open.alberta.ca/dataset/b6f2d99e-30f8-4194-b7eb-76039e9be4d2/resource/063e27cc-b6d1-4dae-8356-44e27304ef78/download/fsoilsands.pdf>) [accessed 21 July 2018].
- Hartsock, J.A., House, M., Clark, M.G., Vitt, D.H., 2021. A comparison of plant communities and water chemistry at Sandhill Wetland to natural Albertan peatlands and marshes. *Ecol. Eng.* 169, 106313 <https://doi.org/10.1016/j.ecoleng.2021.106313>.
- Helbig, M., Humphreys, E.R., Todd, A., 2019. Contrasting Temperature Sensitivity of CO<sub>2</sub> Exchange in Peatlands of the Hudson Bay Lowlands, Canada. *J. Geophys. Res.: Biogeosci.* 124 (7), 2126–2143. <https://doi.org/10.1029/2019JG005090>.
- Howell, T.A., & Dusek, D.A., 1995. Comparison of vapor-pressure-deficit calculation methods-southern high plains.
- Huete, A., Didan, K., Miura, T., Rodriguez, E.P., Gao, X., Ferreira, L.G., 2002. Overview of the radiometric and biophysical performance of the MODIS vegetation indices. *Remote Sens. Environ.* 83 (1–2), 195–213. [https://doi.org/10.1016/S0034-4257\(02\)00096-2](https://doi.org/10.1016/S0034-4257(02)00096-2).
- Huete, A., Justice, C., Liu, H., 1994. Development of vegetation and soil indices for MODIS-EOS. *Remote Sens. Environ.* 49 (3), 224–234.
- Huete, A.R., Liu, H.Q., Batchily, K.V., Van Leeuwen, W.J.D.A., 1997. A comparison of vegetation indices over a global set of TM images for EOS-MODIS. *Remote Sens. Environ.* 59 (3), 440–451.
- Ireson, A.M., Barr, A.G., Johnstone, J.F., Mamet, S.D., van der Kamp, G., Whitfield, C.J., Sagin, J., 2015. The changing water cycle: the Boreal Plains ecozone of Western Canada. *WIREs Water* 2 (5), 505–521. <https://doi.org/10.1002/wat2.1098>.
- Irving, H., 2020, The Impact of LFH Mineral Mix on the Function of Reclaimed Landscapes in the Athabasca Oil Sands Region, Alberta, Canada (Master's thesis, University of Waterloo).
- Jahan, N., Gan, T.Y., 2011. Modelling the vegetation–climate relationship in a boreal mixedwood forest of Alberta using normalized difference and enhanced vegetation indices. *Int. J. Remote Sens.* 32 (2), 313–335.
- Kaimal, J., Finnigan, J., 1994. *Atmospheric Boundary Layer Flows: Their Structure and Measurement*. Oxford University Press, New York.
- Kessel, E.D., Ketcheson, S.J., Price, J.S., 2018. The distribution and migration of sodium from a reclaimed upland to a constructed fen peatland in a post-mined oil sands landscape. *Sci. Total Environ.* 630, 1553–1564. <https://doi.org/10.1016/j.scitotenv.2018.02.253>.
- Ketcheson, S.J., Price, J.S., Sutton, O., Sutherland, G., Kessel, E., Petrone, R.M., 2017. The hydrological functioning of a constructed fen wetland watershed. *Sci. Total Environ.* <https://doi.org/10.1016/j.scitotenv.2017.06.101>.
- Ketcheson, S.J., Price, J.S., Carey, S.K., Petrone, R.M., Mendoza, C.A., Devito, K.J., 2016. Constructing fen peatlands in post-mining oil sands landscapes: Challenges and opportunities from a hydrological perspective. *Earth-Sci. Rev.* <https://doi.org/10.1016/j.earscirev.2016.08.007>.
- Kokkonen, N.A., Laine, A.M., Laine, J., Vasander, H., Kurki, K., Gong, J., Tuittila, E.S., 2019. Responses of peatland vegetation to 15- year water level drawdown as mediated by fertility level. *J. Veg. Sci.* 30 (6), 1206–1216. <https://doi.org/10.1111/jvs.12794>.

- Koropchak, S., Vitt, D.H., Bloise, R., Wieder, R.K., 2012. Fundamental paradigms, foundation species selection, and early plant responses to peatland initiation on mineral soils. In: Vitt, D.H., Bhatti, J. (Eds.), *Restoration and Reclamation of Boreal Ecosystems: Attaining Sustainable Development*. Cambridge University Press, Cambridge, pp. 76–100.
- Kljun, N., Calanca, P., Rotach, M.W., Schmid, H.P., 2004. A Simple parameterisation for flux footprint predictions. *Bound.-Layer. Meteorol.* 112, 503–523.
- Kurz, W.A., Shaw, C.H., Boisvenue, C., Stinson, G., Metsaranta, J., Leckie, D., Neilson, E.T., 2013. Carbon in Canada's boreal forest-A synthesis. *Environ. Rev.* <https://doi.org/10.1139/er-2013-0041>.
- Lafleur, P.M., 1990. Evapotranspiration from sedge-dominated wetland surfaces. *Aquat. Bot.* 37 (4), 341–353. [https://doi.org/10.1016/0304-3770\(90\)90020-L](https://doi.org/10.1016/0304-3770(90)90020-L).
- Laine, A.M., Lindholm, T., Nilsson, M., Kutznetsov, O., Jassey, V.E., Tuittila, E.S., 2021. Functional diversity and trait composition of vascular plant and Sphagnum moss communities during peatland succession across land uplift regions. *J. Ecol.* 109 (4), 1774–1789.
- Lamothe, K.A., Dong, H., Senar, O.E., Teichert, S., Creed, I.F., Kreuzweiser, D.P., ... Venier, L., 2018. Demand for nonprovisioning ecosystem services as a driver of change in the Canadian boreal zone 1. <https://doi.org/10.1139/er-2018-0065>.
- Lavoie, C., Saint-Louis, A., Lachance, D., 2005. Vegetation dynamics on an abandoned vacuum-mined peatland: 5 Years of monitoring. *Wetl. Ecol. Manag.* 13 (6), 621–633. <https://doi.org/10.1007/s11273-005-0126-1>.
- Law, B., Falge, E., Gu, L., Baldocchi, D., Bakwin, P., Berbigier, P., Davis, K., Dolman, A., Falk, M., Fuentes, J., et al., 2002. Environmental controls over carbon dioxide and water vapor exchange of terrestrial vegetation. *Agric. For. Meteorol.* 113, 97–120.
- Lees, K.J., Quaife, T., Artz, R.R.E., Khomik, M., Clark, J.M., 2018. Potential for using remote sensing to estimate carbon fluxes across northern peatlands – A review. February 15 Science of the Total Environment. Elsevier B.V., <https://doi.org/10.1016/j.scitotenv.2017.09.103>.
- Lemmer, M., Rochefort, L., Strack, M., 2020. Greenhouse Gas Emissions Dynamics in Restored Fens After In-Situ Oil Sands Well Pad Disturbances of Canadian Boreal Peatlands. *Front. Earth Sci.* 8, 546.
- Leuning, R., Judd, M.J., 1996. The relative merits of open and closed path analysers for measurement of eddy fluxes. *Glob. Change Biol.* 2, 241–253.
- Limpens, J., Berendse, F., Blodau, C., Canadell, J.G., Freeman, C., Holden, J., Schaeppman-Strub, G., 2008. Peatlands and the carbon cycle: from local processes to global implications – a synthesis. *Biogeosciences* 5, 1475–1491. ([www.biogeosciences.net/5/1475/2008/](http://www.biogeosciences.net/5/1475/2008/)).
- Litvak, M., Miller, S., Wofsy, S.C., Goulden, M., 2003. Effect of stand age on whole ecosystem CO<sub>2</sub> exchange in the Canadian boreal forest. *J. Geophys. Res.: Atmos.* 108 (3), 8225. <https://doi.org/10.1029/2001jd000854>.
- Loisel, J., Yu, Z., 2013. Surface vegetation patterning controls carbon accumulation in peatlands. *Geophys. Res. Lett.* 40 (20), 5508–5513. <https://doi.org/10.1002/grl.50744>.
- Lund, M., Lafleur, P.M., Roulet, N.T., Lindroth, A., Christensen, T.R., Aurela, M., Nilsson, M.B., 2010. Variability in exchange of CO<sub>2</sub> across 12 northern peatland and tundra sites. *Glob. Change Biol.* 16 (9), 2436–2448.
- MacKenzie, M.D., Quideau, S.A., 2010. Microbial community structure and nutrient availability in oil sands reclaimed boreal soils. *Appl. Soil Ecol.* 44 (1), 32–41. <https://doi.org/10.1016/j.apsoil.2009.09.002>.
- Maestre, F.T., Bautista, S., Cortina, J., Bellot, J., 2001. Potential for using facilitation by grasses to establish shrubs on a semiarid degraded steppe. *Ecol. Appl.* 11 (6), 1641–1655.
- Marshall, I.B., Schut, P., Ballard, M. (compilers), 1999. Canadian ecodistrict climate normals for Canada 1961–1990. A national ecological framework for Canada: Attribute Data. Environmental Quality Branch, Ecosystems Science Directorate, Environment Canada and Research Branch, Agriculture and Agri-Food Canada., Ottawa/Hull.
- Messner, Lewis, 2019. Approaches for creating sustainable biomass production in a reclaimed. Thesis.
- Mkhabela, M.S., Amiro, B.D., Barr, A.G., Black, T.A., Hawthorne, I., Kidston, J., Zha, T., 2009. Comparison of carbon dynamics and water use efficiency following fire and harvesting in Canadian boreal forests. *Agric. For. Meteorol.* 149 (5), 783–794.
- Miura, T., Huete, A.R., Van Leeuwen, W.J.D., Didan, K., 1998. Vegetation detection through smoke-filled AVIRIS images: An assessment using MODIS band passes. *J. Geophys. Res.: Atmos.* 103 (D24), 32001–32011.
- Morison, M.Q., Petrone, R.M., Wilkinson, S.L., Green, A., Waddington, J.M., 2020. Ecosystem scale evapotranspiration and CO<sub>2</sub> exchange in burned and unburned peatlands: Implications for the ecophysiological resilience of carbon stocks to wildfire. *Ecology* 13 (2), e2189.
- Nicholls, E.M., Carey, S.K., Humphreys, E.R., Clark, M.G., Drewitt, G.B., 2016. Multi-year water balance assessment of a newly constructed wetland, Fort McMurray, Alberta. *Hydro. Process.* 30 (16), 2739–2753.
- Nijp, J.J., Limpens, J., Metselaar, K., Peichl, M., Nilsson, M.B., van der Zee, S.E., Berendse, F., 2015. Rain events decrease boreal peatland net CO<sub>2</sub> uptake through reduced light availability. *Glob. Change Biol.* 21 (6), 2309–2320.
- Naeth, M.A., Wilkinson, S.R., Mackenzie, D.D., Archibald, H.A., & Powter, C.B., 2013. Potential of LFH Mineral Soil Mixes for Reclamation of Forested Lands in Alberta. Retrieved from (<http://hdl.handle.net/10402/era.17507>).
- Nilsson, M., Sagerfors, J., Buffam, I., Laudon, H., Eriksson, T., Grelle, A., Lindroth, A., 2008. Contemporary carbon accumulation in a boreal oligotrophic minerogenic mire - A significant sink after accounting for all C-fluxes. *Glob. Change Biol.* 14 (10), 2317–2332. <https://doi.org/10.1111/j.1365-2486.2008.01654.x>.
- Nugent, K.A., Strachan, I.B., Roulet, N.T., Strack, M., Frolking, S., Helbig, M., 2019. Prompt active restoration of peatlands substantially reduces climate impact. *Environ. Res. Lett.* 14 (12), 124030.
- Nugent, K.A., Strachan, I.B., Strack, M., Roulet, N.T., Rochefort, L., 2018. Multi-year net ecosystem carbon balance of a restored peatland reveals a return to carbon sink. *Glob. Change Biol.* 24 (12), 5751–5768. <https://doi.org/10.1111/gcb.14449>.
- Nwaishi, F., Petrone, R.M., Macrae, M.L., Price, J.S., Strack, M., Andersen, R., 2016. Preliminary assessment of greenhouse gas emissions from a constructed fen on post-mining landscape in the Athabasca oil sands region, Alberta, Canada. *Ecol. Eng.* 95, 119–128. <https://doi.org/10.1016/j.ecoleng.2016.06.061>.
- Nwaishi, F., Petrone, R.M., Price, J.S., Andersen, R., 2015a. Towards Developing a Functional-Based Approach for Constructed Peatlands Evaluation in the Alberta Oil Sands Region, Canada. *Wetlands* 35 (2), 211–225. <https://doi.org/10.1007/s13157-014-0623-1>.
- Nwaishi, F., Petrone, R.M., Price, J.S., Ketcheson, S.J., Slawson, R., Andersen, R., 2015b. Impacts of donor-peat management practices on the functional characteristics of a constructed fen. *Ecol. Eng.* <https://doi.org/10.1016/j.ecoleng.2015.04.038>.
- Padilla, F.M., Ortega, R., Sánchez, J., Pugnaire, F.I., 2009. Rethinking species selection for restoration of arid shrublands. *Basic Appl. Ecol.* 10 (7), 640–647.
- Peichl, M., Gažović, M., Vermeij, I., De Goede, E., Sonntag, O., Limpens, J., Nilsson, M.B., 2018. Peatland vegetation composition and phenology drive the seasonal trajectory of maximum gross primary production. *Sci. Rep.* 8 (1), 1–11.
- Petrone, R., Chasmer, L., Hopkinson, C., Silins, U., Landhäusser, S., Kljun, N., Devito, K., 2015. Effects of harvesting and drought on CO<sub>2</sub> and H<sub>2</sub>O fluxes in an aspen-dominated western boreal plain forest: early chronosequence recovery. *Can. J. Res. Can. J. Res.* 4519. <https://doi.org/10.1139/cjfr-2014-0253>.
- Petrone, R.M., Silins, U., Devito, K.J., 2007. Dynamics of evapotranspiration from a riparian pond complex in the Western Boreal forest, Alberta, Canada. *Hydro. Process.* 21 (11), 1391–1401. <https://doi.org/10.1002/hyp.6298>.
- Petrone, Richard, M., Price, J.S., Waddington, J.M., Von Waldow, H., 2004. Surface moisture and energy exchange from a restored peatland, Québec, Canada. *J. Hydrol.* 295 (1–4), 198–210. <https://doi.org/10.1016/j.jhydrol.2004.03.009>.
- Petrone, Richard, M., Waddington, J.M., Price, J.S., 2003. Ecosystem-scale flux of CO<sub>2</sub> from a restored vacuum harvested peatland. *Wetl. Ecol. Manag.* Vol. 11.
- Petrone, Richard M., Waddington, J.M., Price, J.S., 2001. Ecosystem scale evapotranspiration and net CO<sub>2</sub> exchange from a restored peatland. *Hydro. Process.* 15 (14), 2839–2845. <https://doi.org/10.1002/hyp.475>.
- Pinno, B.D., Hawkes, V.C., 2015. Temporal trends of ecosystem development on different site types in reclaimed boreal forests. *Forests* 6 (6), 2109–2124.
- Poscente, M., & Charette, T. (2011). Criteria and indicator framework for oil sands mine reclamation. In Proceedings of the Sixth International Conference on Mine Closure (pp. 455–462). Australian Centre for Geomechanics, Perth.
- Poulin, M., Andersen, R., Rochefort, L., 2013. A new approach for tracking vegetation change after restoration: A case study with peatlands. *Restor. Ecol.* 21 (3), 363–371. <https://doi.org/10.1111/j.1526-100X.2012.00889.x>.
- Pouliot, R., Rochefort, L., Graf, M.D., 2012. Impacts of oil sands process water on fen plants: Implications for plant selection in required reclamation projects. *Environ. Pollut.* <https://doi.org/10.1016/j.envpol.2012.03.050>.

- Price, J.S., McLaren, R.G., Rudolph, D.L., 2010. Landscape restoration after oil sands mining: Conceptual design and hydrological modelling for fen reconstruction. *Int. J. Min., Reclam. Environ.* 24 (2), 109–123. <https://doi.org/10.1080/17480930902955724>.
- Price, J., Rochefort, L., Quinty, F., 1998. Energy and moisture considerations on cutover peatlands: surface microtopography, mulch cover and Sphagnum regeneration. *Ecol. Eng.* 10 (4), 293–312.
- Prentice, T.M. (2020). Quantifying the Influence of Soil Prescriptions on Ecosystem Processes in Reclaimed Forests of Varying Age in a Post-Oil Sands Landscape in the Athabasca Oil Sands Region, Alberta, Canada (Master's thesis, University of Waterloo).
- Province of Alberta, 2020. Environmental Protection and Enhancement Act - Chapter/Regulation: E-12 RSA 2000. Alberta Queen's Printer from ([https://www.qp.alberta.ca/1266.cfm?page=E12.cfm&leg\\_type=Acts&isbncln=9780779822706](https://www.qp.alberta.ca/1266.cfm?page=E12.cfm&leg_type=Acts&isbncln=9780779822706)).
- Pulliaainen, J., Aurela, M., Laurila, T., Aalto, T., Takala, M., Salminen, M., Vesala, T., 2017. Early snowmelt significantly enhances boreal springtime carbon uptake. *Atmos. Planet. Sci.* 17. <https://doi.org/10.1073/pnas.1707889114>.
- Purdy, B.G., Macdonald, S.E., Lieffers, V.J., 2005. Naturally saline boreal communities as models for reclamation of saline oil sand tailings. *Restor. Ecol.* 13 (4), 667–677. <https://doi.org/10.1111/j.1526-100X.2005.00085.x>.
- Rankin, T., Strachan, I.B., Strack, M., 2018. Carbon dioxide and methane exchange at a post-extraction, unrestored peatland. *Ecol. Eng.* 122, 241–251. <https://doi.org/10.1016/j.ecoleng.2018.06.021>.
- Reichstein, M., Falge, E., Baldocchi, D., Papale, D., Aubinet, M., Berbigier, P., Valentini, R., 2005. On the separation of net ecosystem exchange into assimilation and ecosystem respiration: review and improved algorithm. *Glob. Change Biol.* 11 (9), 1424–1439.
- Rezanezhad, F., Andersen, R., Pouliot, R., & Price, J.S., 2012, How Fen Vegetation Structure Affects the Transport of Oil Sands Process-affected Waters, 557–570. <https://doi.org/10.1007/s13157-012-0290-z>.
- Rodriguez-Iturbe, I., & Porporato, A. (2004). Ecohydrology of Water-Controlled Ecosystems: soil moisture and plant dynamics.
- Rochefort, L., Quinty, F., Campeau, S., Johnson, K., Malterer, T., 2003. North American approach to the restoration of Sphagnum dominated peatlands. *Wetl. Ecol. Manag.* 11 (1), 3–20.
- Rochefort, L., 2000. Sphagnum: a keystone genus in habitat restoration. *Bryologist* 103 (3), 503–508.
- Rooney, R.C., Bayley, S.E., Schindler, D.W., 2012. Oil sands mining and reclamation cause massive loss of peatland and stored carbon. *Proc. Natl. Acad. Sci. USA* 109 (13), 4933–4937. <https://doi.org/10.1073/pnas.1117693108>.
- Roulet, N.T., Lafleur, P.M., Richard, P.J.H., Moore, T.R., Humphreys, E.R., Bubier, J., 2007. Contemporary carbon balance and late Holocene carbon accumulation in a northern peatland. *Glob. Change Biol.* 13, 397–411.
- Rowland, S.M., Prescott, C.E., Grayston, S.J., Quideau, S.A., Bradfield, G.E., 2009. Recreating a Functioning Forest Soil in Reclaimed Oil Sands in Northern Alberta: An Approach for Measuring Success in Ecological Restoration. *J. Environ. Qual.* 38 (4), 1580–1590. <https://doi.org/10.2134/jeq2008.0317>.
- Samaritani, E., Siegenthaler, A., Yli-Petäys, M., Buttler, A., Christin, P.A., Mitchell, E.A., 2011. Seasonal net ecosystem carbon exchange of a regenerating cutaway bog: How long does it take to restore the C-sequestration function? *Restor. Ecol.* 19 (4), 480–489.
- Semeraro, V., Vacchiano, G., Aretano, R., Ascoli, D., 2019. Application of vegetation index time series to value fire effect on primary production in a southern European rare wetland. *Ecol. Eng.* 134, 9–17. <https://doi.org/10.1016/j.ecoleng.2019.04.004>.
- Scarlett, S.J., Petrone, R.M., Price, J.S., 2017. Controls on plot-scale evapotranspiration from a constructed fen in the Athabasca Oil Sands Region, Alberta. *Ecol. Eng.* 100, 199–210. <https://doi.org/10.1016/j.ecoleng.2016.12.020>.
- Scarlett, S.J., Price, J.S., 2019. The influences of vegetation and peat properties on the hydrodynamic variability of a constructed fen, Fort McMurray, Alberta. *Ecol. Eng.* 139, 105575 <https://doi.org/10.1016/j.ecoleng.2019.08.005>.
- Schubert, P., Eklundh, L., Lund, M., Nilsson, M., 2010. Estimating northern peatland CO<sub>2</sub> exchange from MODIS time series data. *Remote Sens. Environ.* 114 (6), 1178–1189. <https://doi.org/10.1016/j.rse.2010.01.005>.
- Scheffer, M., 2010. Foreseeing tipping points. *Nature* 467 (7314), 411–412.
- Seyfried, M.S., Grant, L.E., Du, E., Humes, K., 2005. Dielectric loss and calibration of the Hydra Probe soil water sensor. *Vadose Zone J.* 4 (4), 1070–1079.
- Shih, J.G., Finkelstein, S.A., 2008. Range dynamics and invasive tendencies in *Typha latifolia* and *Typha angustifolia* in eastern North America derived from herbarium and pollen records. *Wetlands* 28 (1), 1–16.
- Simhayov, R.B., Price, J.S., Smeaton, C.M., Parsons, C., Rezanezhad, F., Van Cappellen, P., 2017. Solute pools in Nikanotee Fen watershed in the Athabasca oil sands region. *Environ. Pollut.* 225, 150–162. <https://doi.org/10.1016/j.envpol.2017.03.038>.
- Smerdon, B.D., Mendoza, C.A., Devito, K.J., 2008. Influence of subhumid climate and water table depth on groundwater recharge in shallow outwash aquifers. *Water Resour. Res.* 44 (8), W08427.
- Spennato, H.M., Ketcheson, S.J., Mendoza, C.A., Carey, S.K., 2018. Water table dynamics in a constructed wetland, Fort McMurray, Alberta. *Hydrol. Process.* 32 (26), 3824–3836.
- Strack, Maria, Keith, A.M., Xu, B., 2014. Growing season carbon dioxide and methane exchange at a restored peatland on the Western Boreal Plain. *Ecol. Eng.* 64, 231–239. <https://doi.org/10.1016/j.ecoleng.2013.12.013>.
- Strack, M., Zuback, Y.C.A., 2013. Annual carbon balance of a peatland 10 yr following restoration. *Biogeosciences* 10 (5), 2885–2896.
- Strack, M., Waddington, J.M., Rochefort, L., Tuittila, E.S., 2006. Response of vegetation and net ecosystem carbon dioxide exchange at different peatland microforms following water table drawdown. *J. Geophys. Res.: Biogeosci.* 111 (2) <https://doi.org/10.1029/2005JG000145>.
- Straker, J.R., Carey, S.K., Petrone, R.M., Baker, T.D., & Strilesky, S.L., 2019, Developing a Functional Approach to Assessment of Landscape Capability: Utilizing Ecosystem Water and Carbon Nutrient Fluxes as Integrated Measures of Reclamation Performance.
- Strilesky, S.L., Humphreys, E.R., Carey, S.K., 2017. Forest water use in the initial stages of reclamation in the Athabasca Oil Sands Region. *Hydrol. Process.* 31 (15), 2781–2792. <https://doi.org/10.1002/hyp.11220>.
- Sutton, O.F., 2021, Projecting the Hydrological and Geochemical Evolution of a Constructed Fen Watershed in the Athabasca Oil Sands Region, Alberta, Canada. UWSpace. (<http://hdl.handle.net/10012/16965>).
- Sutton, O.F., & Price, J.S., 2020a, Modelling the hydrologic effects of vegetation growth on the long-term trajectory of a reclamation watershed. <https://doi.org/10.1016/j.scitotenv.2020.139323>.
- Sutton, O.F., Price, J.S., 2020b, Soil moisture dynamics modelling of a reclaimed upland in the early post-construction period. *Sci. Total Environ.* 718, 134628 <https://doi.org/10.1016/j.scitotenv.2019.134628>.
- Tariq, S., Nawaz, H., Ul-Haq, Z., Mehmood, U., 2021. Investigating the relationship of aerosols with enhanced vegetation index and meteorological parameters over Pakistan. *Atmos. Pollut. Res.* 12 (6), 101080.
- Tuittila, E.S., Komulainen, V.M., Vasander, H., Laine, J., 1999. Restored cut-away peatland as a sink for atmospheric CO<sub>2</sub>. *Oecologia* 120 (4), 563–574.
- Thompson, C., Mendoza, C.A., Devito, K.J., 2017. Potential influence of climate change on ecosystems within the Boreal Plains of Alberta. *Hydrol. Process.* 31 (11), 2110–2124. <https://doi.org/10.1002/hyp.11183>.
- Trites, M., Bayley, S.E., 2009. Vegetation communities in continental boreal wetlands along a salinity gradient: Implications for oil sands mining reclamation. *Aquat. Bot.* 91 (1), 27–39. <https://doi.org/10.1016/j.aquabot.2009.01.003>.
- Vasander, H., Kettunen, A., 2006. Carbon in boreal peatlands. *Boreal Peatland Ecosystems*. Springer, Berlin, Heidelberg, pp. 165–194.
- Vermote, E., Justice, C., Claverie, M., Franch, B., 2016. Preliminary analysis of the performance of the Landsat 8/OLI land surface reflectance product. *Remote Sens. Environ.* 185, 46–56.
- Vitt, D.H., Glaeser, L.C., House, M., Kitchen, S.P., 2020. Structural and functional responses of *Carex aquatilis* to increasing sodium concentrations. *Wetl. Ecol. Manag.* 28 (5), 753–763. <https://doi.org/10.1007/s11273-020-09746-9>.
- Vitt, D.H., House, M., Hartsock, J.A., 2016. Sandhill fen, an initial trial for wetland species assembly on in-pit substrates: Lessons after three years. *Botany* 94 (11), 1015–1025. <https://doi.org/10.1139/cjb-2015-0262>.
- Volik, O., Petrone, R., Kessel, E., Green, A., Price, J., 2021. Understanding the peak growing season ecosystem water-use efficiency at four boreal fens in the Athabasca Oil Sands Region. *Hydrol. Process.* <https://doi.org/10.1002/hyp.14323>.

- Volik, O., Elmes, M., Petrone, R., Kessel, E., Green, A., Cobbaert, D., Price, J., 2020a. Wetlands in the athabasca oil sands region: The nexus between wetland hydrological function and resource extraction. *Environ. Rev.* 28 (3), 246–261. <https://doi.org/10.1139/er-2019-0040>.
- Volik, O., Petrone, R.M., Quanz, M., Macrae, M.L., Rooney, R., Price, J.S., 2019. Environmental Controls on CO<sub>2</sub> Exchange along a Salinity Gradient in a Saline Boreal Fen in the Athabasca Oil Sands Region. *Wetlands* 1–14.
- Volik, O., Petrone, R.M., Wells, C.M., 2018. Impact of Salinity, Hydrology and Vegetation on Long-Term Carbon Accumulation in a Saline Boreal Peatland and its Implication for Peatland Reclamation in the Athabasca Oil Sands Region. *Wetlands* 38 (2018), 373–382. <https://doi.org/10.1007/s13157-017-0974-5>.
- Waddington, J.M., Strack, M., Greenwood, M.J., 2010. Toward restoring the net carbon sink function of degraded peatlands: Short-term response in CO<sub>2</sub> exchange to ecosystem-scale restoration. *J. Geophys. Res.* 115 (G1), 1008. <https://doi.org/10.1029/2009jg001090>.
- Webb, E.K., Pearman, G., Leuning, R., 1980. Correction of flux measurements for density effects due to heat and water vapour transfer. *Q. J. R. Meteorol. Soc.* 106, 85–100.
- Wells, C., Ketcheson, S., Price, J., 2017. Hydrology of a wetland-dominated headwater basin in the Boreal Plain, Alberta, Canada. *J. Hydrol.* 547, 168–183.
- Winslow, L.A., Zwart, J.A., Batt, R.D., Dugan, H.A., Woolway, R.I., Corman, J.R., Read, J.S., 2016. LakeMetabolizer: An R package for estimating lake metabolism from free- water oxygen using diverse statistical models. *Inland Waters*.
- Wutzler, T., Lucas-Moffat, A., Migliavacca, M., Knauer, J., Sickel, K., Šigut, L., et al., 2018. Basic and extensible post-processing of eddy covariance flux data with R EddyProc. *Biogeosciences* 15 (16), 5015–5030. <https://doi.org/10.5194/bg-15-5015-2018>.
- Yu, Z.C., 2012. Northern peatland carbon stocks and dynamics: a review. *Biogeosciences* 9, 4071–4085. <https://doi.org/10.5194/bg-9-4071-2012>.
- Zhang, T., Gong, W., Wang, W., Ji, Y., Zhu, Z., Huang, Y., 2016. Ground level PM<sub>2.5</sub> estimates over China using satellite-based geographically weighted regression (GWR) models are improved by including NO<sub>2</sub> and enhanced vegetation index (EVI). *Int. J. Environ. Res. Public Health* 13 (12), 1215. <https://doi.org/10.3390/ijerph13121215>.